
POTSDAM-INSTITUT FÜR KLIMAFOLGENFORSCHUNG



**Originally published as:**

**Layritz, L. S., Dolganova, I., Finkbeiner, M., Luderer, G., Penteado, A. T., Ueckerdt, F., Repke, J.-U. (2021):** The potential of direct steam cracker electrification and carbon capture & utilization via oxidative coupling of methane as decarbonization strategies for ethylene production. - Applied Energy, 296, 117049.

**DOI**: 10.1016/j.apenergy.2021.117049

# The potential of direct steam cracker electrification and carbon capture & utilization via oxidative coupling of methane as decarbonization strategies for ethylene production

Lucia S. Layritz [a, b, c, *], Iulia Dolganova [c], Matthias Finkbeiner [c], Gunnar Luderer [a], Alberto T. Penteado [b], Falko Ueckerdt [a], Jens–Uwe Repke [b]

[a] *Potsdam Institute for Climate Impact Research, Telegraphenberg A 31 14473 Potsdam*
[b] *Process Dynamics and Operations Group, Faculty for Process Engineering, Technische Universität Berlin, Sekretariat KWT 9, Straße des 17. Juni 135 10623 Berlin*
[c] *Sustainable Engineering Group, Faculty for Process Engineering, Technische Universität Berlin, Straße des 17. Juni 135 10623 Berlin*
[*] *Corresponding author*

**Abstract**

Ethylene is one of the most important building blocks in the chemical industry, making its decarbonization a natural starting point for achieving emission targets of the industrial sector. We here present an in–depth analysis of carbon and energy flows of two main strategies that could potentially reduce emissions from ethylene production: (i) direct electrification of heat supply in the traditional steam cracking process and (ii) indirect electrification through a novel production route based on Power-to-Gas and Oxidative Coupling of Methane (OCM–PtG). By calculating carbon footprints of all processes as a function of electricity carbon intensity, we show that fuelling the steam cracker with renewable electricity can achieve a maximal emission reduction of 30% while OCM–PtG can achieve a net–zero emission production process if electricity supply is completely decarbonized and resulting products are at least partially recycled at the end of their life cycle. An integrated analysis within an economy–wide, global climate policy scenario shows that these conditions are likely to be met only after 2030 even under very stringent climate policy in line with the climate targets of the Paris agreement. If not met, OCM–PtG can actually increase the carbon footprint of ethylene. We also show that OCM–PtG is currently not cost–competitive, but can become so under suitable boundary conditions. It becomes clear that policy instruments that support the market introduction of carbon capture utilization technologies like OCM–PtG are only justified, if conditions are ensured that enable a positive mitigation potential over their life cycle.

*Keywords:* Industry Decarbonization, Carbon Capture and Utlization (CCU), Power-to-Gas, Steam Cracking, Oxidative Coupling of Methane, Carbon Footprint

## 1. Introduction

The climate targets set by the international community under the Paris agreement require anthropogenic greenhouse gas (GHG) emissions to approach net–zero by the second half of the century [1]. This calls for a rapid decarbonization of all economic sectors, including so far underresearched subsectors such as the chemical industry. Despite previous studies showing that the decarbonization [1] of the chemical sector will not be achieved by a transformation of the energy system alone [2, 3], sufficient knowledge about strategies that are able to fulfill this goal are lacking so far [4]. Nevertheless, current mitigation targets for the industrial sector imply a drastic cut in emissions by all its subsectors including the chemical. In the European Union, the sector targets for the industry call for a 83% to 87% reduction in 2050 compared to 1990 [5]. In Germany, where the chemical industry is the third largest industrial subsector, a 50% reduction is planned by 2030 (rel. to 1990), which translates into a 27% reduction of 2018 levels [6]. Hence, the industry is in need of information about its technological options for decarbonization.

Two general strategies are found in the literature for reducing the emissions of industrial processes, both aiming at the substitution of fossil fuels through low–carbon electricity, assumed to be emissions–free: the *direct electrification* of process heat production itself through electric furnaces and the *indirect electrification* through electrochemically produced products, fuels, or feedstock from still cheap, abundant and less problematic feedstocks such as $H_2O$, $N_2$ or $CO_2$ (often termed carbon capture and utilization (CCU)) [7–10].

Steam cracking (SC), i.e. the thermal processing of fossil feedstock into smaller–sized high value chemicals (HVCs), is the most energy intensive process in the industry [11, 12], making its decarbonization a priority. As the products of steam cracking, most prominently ethylene, serve as the major building blocks of the polymer industry, the critical discourse regarding the broader environmental impacts of plastic products adds further relevance.

Direct electrification of steam cracking is currently proposed by a number of chemical companies, among others BASF, Dow Chemicals or LyondellBasell, while a detailed investigation into the expected emission cuts has not yet occured [13–15].

CCU, on the other side has received massive attention lately as a potential climate mitigation strategy, both in material and synthetic fuel production. A key technology for CCU is the Power–to–Gas (PtG) technology, wherein electricity is used to produce high–energetic hydrogen gas via water electrolysis. This can subsequently be reacted with $CO_2$ to form methane as a stable, versatile and already established energy carrier to be used both as a fuel and feedstock [16–20].

[1] by *decarbonization* we refer to a transformation process that reduces the use of fossil carbon in the economy to achieve an economy–wide balance of carbon sources and sinks. We acknowledge that the term in its literal meaning might be contradictory in the context of the chemical industry, but will regardlessly use it due to its established use within the mitigation literature

PtG has gained significant popularity during the last years as a potential strategy to produce low-carbon fuels [7, 16–18, 21]. Besides fostering the integration of renewables, its key strengths are its versatile application in many different sectors such as energy storage, mobility or industry [22]. The high electrolyzer costs and low system efficiencies of around 55% are the main barriers to a large scale implementation of PtG systems under current economic conditions [17, 22, 23]. However, both are projected to improve in the future, therefore PtG is expected to play a substantial role in many low-emission scenarios and in industry decarbonization [7, 24, 25].

Nevertheless, doubt have been formulated regarding the environmental and economic potential of CCU processes such as PtG in the chemical industry [19, 26, 27]. A consensus is slowly forming that the potential benefits of CCU can not be generalized across the industry and rather a case–to–case evaluation is necessary, assessing the life–cycle emissions of the product and process in question [28, 29]. Therefore life cycle analyses of CCU processes are currently emerging, such as those by von der Assen and Bardow [30] or Meys et al. [31]. However, such analyses are still missing for many key base chemicals.

Ethylene is the base monomer for around 60% of the world's polymers, and its production volumes are therefore expected to grow in line with the substantial plastics demand increase projected for the future [32]. Consequently, detailed analyses about the emission saving potential and feasibility of different mitigation strategies proposed are urgently needed.

One such proposed alternative production process is Oxidative Coupling of Methane (OCM) [9, 33, 34]. The production of ethylene via oxidative coupling of fossil methane has attracted industrial and academic interests ever since its first introduction in the 1980s [35]. However, the technical implementation has been hindered by a low selectivity and a number of undesired side reactions such as the full oxidation of methane, ethane and ethylene to carbon monoxide and $CO_2$, resulting in low ethylene yields. Therefore the search for more selective catalysts is a major area of research in OCM development. A first commercial demonstration plant run by Siluria Technologies in Texas, U.S. has started operation in 2014 [36, 37].

In the light of tighter environmental regulations and concerns over climate change, OCM has also attracted attention due to its potential environmental superiority. Stangland [38] points out that OCM has both a higher thermodynamic and carbon efficiency than steam cracking. Additionally, OCM can utilize biogas as a renewable feedstock [39]. OCM as a CCU process has already been discussed in the mitigation literature to some extent [9, 33, 34] but has so far not been demonstrated technically. Accordingly, it has not yet been subjected to a thorough analysis of its mitigation potential, a gap we want to close with this study.

This paper thus presents a novel ethylene production pathway based on OCM and the PtG technology. We provide a detailed Aspen Plus model of the central process steps of this novel process and compare it to conventional steam cracking and a complete electrification thereof by calculating their complete life–cycle emissions

under different levels of grid electricity decarbonization. We investigate the potential role of the OCM–PtG process in a zero-carbon economy further by assessing the development of emissions and also of main cost components of all three technologies under different climate policy scenarios. Our results therefore provide insights into the general viability of different decarbonization strategies for the chemical sector and more specifically for ethylene production.

## 2. Material and Methods

### *2.1. Carbon footprints*

We calculate cradle-to-gate and cradle-to-grave carbon footprints for conventional steam cracking, electrified steam cracking and OCM–PtG as a function of grid electricity carbon intensity, following the methodology of the International Organization for Standardization [40–42]. We first construct our product systems based on cradle–to–gate processes as depicted in Figure 1. Appendix A.1 provides further technical background on all systems.

Steam cracking produces a range of HVCs next to ethylene as well as high-energetic gases such as $H_2$ and $CH_4$. Therefore, we perform a system expansion based on an initial functional unit of 1 metric ton (t) of ethylene to ensure all product systems produce the same amount of valuable output. For this, we establish that all co-produced high-energetic off–gases that are not used internally are converted to electricity in a gas–fired power plant in all process systems. The final functional unit is comprised of 1t ethylene, 0.55 t propylene, 0.267 t benzene and 4.32 MWh electricity. To investigate the relevance of off–gas fate on the overall results, we also design alternative systems in which the off–gases are either assumed to substitute natural gas or residential heating oil.

In the initial design of the OCM-PtG plant we assume an alkaline electrolyzer that is running on constant load with an efficiency $\eta_{el}$ of $0.72\,\mathrm{MWh_{H_2}\,MWh_{el}^{-1}}$ based on Milanzi et al. [24]. The oxygen produced during electrolysis is partly used in the OCM reaction. For the economic analysis we also investigate systems that run in flexible load to take advantage of fluctuating electricity prices. Here we use a polymer electrolyte membrane electrolyzer that is better suited for flexible load. The integration of hydrogen storage facilities in the model is beyond the scope of this work and is therefore not taken into account in the flexible systems.

Emissions from the plant construction phase are not considered as these have been shown to be negligible in comparable studies [30]. Upstream emission associated with the catalyst production are also neglected as no data was available and those from transport are not included as the product system lacks sufficient geographical definition. Emissions from (waste) water treatment are neglected in the OCM process since equally detailed data is not available for steam cracking and inclusion would compromise the comparability between the two processes.

While previous research indicates, that the amount of fugitive methane emissions (FME) from methane–processing plants might be quite significant, there is little

experience in determining the actual amount [43, 44]. As in our case no experimental data of FME is available, we perform a sensitivity analysis on its possible effect by assuming escape rates between 0.01 % to 2.5 % of the inflow stream to the OCM reactor.

In a second step we calculate cradle–to–grave emissions for different manufacturing routes and end–of–life (EoL) strategies, which are the same for all processes. Due to the versatile uses of ethylene, we chose polyvinylchloride (PVC) pipes, polyethylene (PE) bottles and PE foam as representative final products and considered recycling and incineration as the most common EoL strategies for plastic products.

We deduce all data either from the literature or from GaBi, database version 8.7 [45]. The notable exception is the methanation and OCM process, data on which are derived from the Aspen Plus process model we designed for this study and is described in section 2.2. Appendix A.2 gives detailed information about data sources as well as the underlying assumptions during the constructing of product systems.

In the subsequent impact assessment all relevant GHG emissions are converted to $CO_2$ equivalents, the impact category being $GWP_{100}$. In the case of FME this is done based on Stocker [46] and in the case of direct combustion processes based on Eggleston [43]. For GaBi [45] we choose CML 2001 as the characterization method [47].

For comparison of the different processes we define the emission saving potential (ESP) as

$$ESP = \sum E \text{ (conventional process)} - \sum E \text{ (alternative process)} \tag{1}$$

where $E$ are cradle–to-gate emissions in $\mathrm{t_{CO_2eq}\,t_{Eth}^{-1}}$. As manufacturing and and–of–life steps are identical for all process system, they do not affect the ESP. A process is beneficial if the ESP is positive.

We also define the relative ESP as

$$ESP_{rel} = \frac{ESP \text{ (alternative process)}}{E \text{ (SC)}} \tag{2}$$

### *2.2. AspenPlus Model*

We designed a simulation of the novel OCM-PtG process, as the PtG configuration is novel to this study and no empirical data is available on its mass and energy flows. The simulation model is implemented in the software Aspen Plus 10.1 and overall emissions of the process are extracted by a Python script linked to the ActiveX Automation Server of the AspenPlus program [48]. The emissions are then minimized further by varying the operating parameters.

The simulation model for the OCM process has been developed using the PENG-ROB Property Method of Aspen Plus, which is based on the Peng-Robinson Equation of

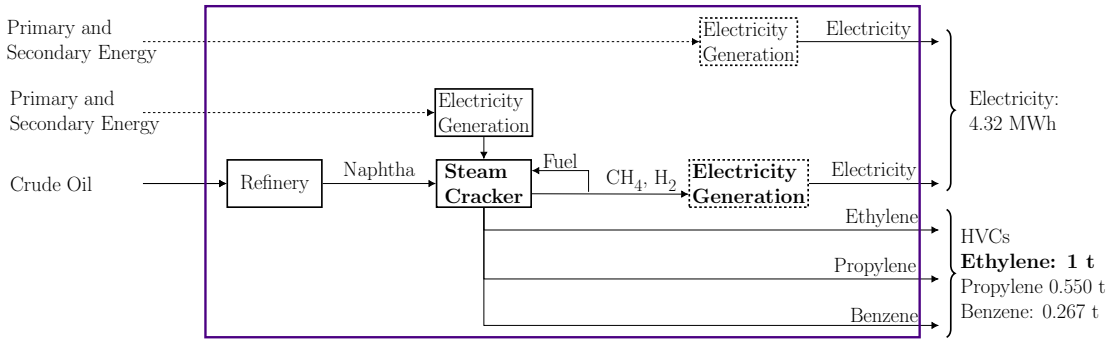


(a) Conventional Steam Cracking: The process uses Naphtha as feedstock. Besides HVCs, it produces high–energetic gases that are energetically recycled internally to meet the high heat demand needed to achieve the required cracking temperature of 759°C – 1000°C.

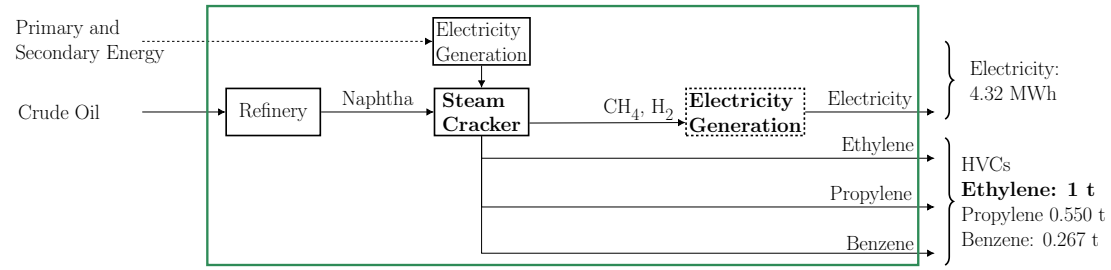


(b) Electrified Steam Cracking: The furnace is substituted by an electric heater, raising the electricity demand of the cracker. In return, high-energetic off-gases are released.

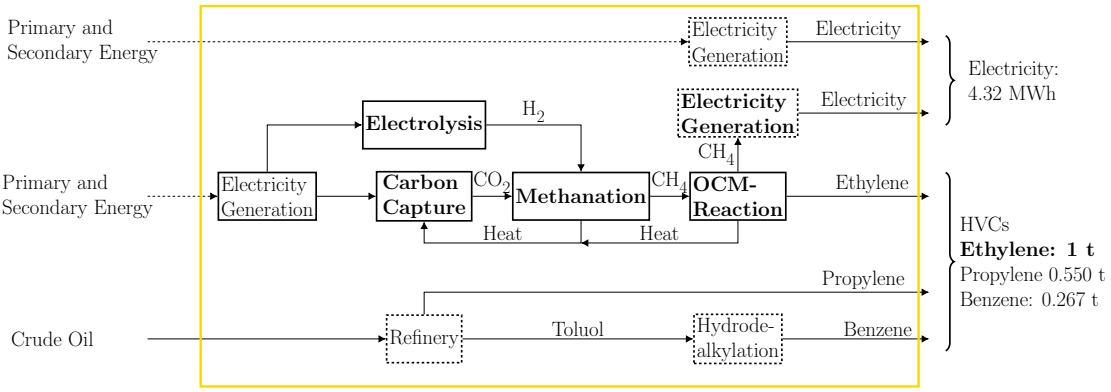


(c) OCM–PtG: Heat from the exothermic OCM-reaction is reused in carbon capture and methanation. Unreacted methane is exported. Oxygen produced in water electrolysis is reused in the OCM-reaction (not shown in figure).

Figure 1: Final product systems. System expansion processes are depicted as dashed boxes. Dashed arrows indicate flows that are influences by the electricity grid carbon intensity. For a detailed technical description of all processes see Appendix A.1

State and the full set of binary parameters available from Aspen and NIST databanks [49]. This model has been previously utilized to simulate a biogas-based OCM process [39], wherein model validations by comparison with experimental data are shown for main pure component properties as well as for phase-equilibria. The OCM reaction is modeled at 10 bar.

The methanation reactors are considered to be adiabatic equilibrium reactors and modeled by a Gibbs reactor (RGIBBS in Aspen Plus), with feed exhibiting a $H_2/CO_2$-ratio of 3 at 10 bar and 220 °C. The OCM reactors are modeled as adiabatic plug-flow reactors (RPLUG in Aspen Plus) with kinetics proposed by Friedel et al. [50] and the feed containing a $CH_4/O_2$-ratio of 8 and a temperature of at least 650 °C. Carbon capture with amines is a relatively well understood process and data for energy demands and costing are available, so that $CO_2$ removal by scrubbing with monoethanolamine 30wt % aqueous solution is modeled as a black-box separator, which removes all the $CO_2$ and imposes some hydrocarbon losses estimated based on previous simulations by Penteado et al. [39]. This avoids the simulation of the absorption–desorption cycle with the rigorous electrolyte non–random two–liquid model, which is computationally expensive. The final hydrocarbon split is modeled by two equilibrium columns (RadFrac in Aspen Plus) to represent the demethanizer and C2-splitter distillation columns.

The model process is designed for an initial electrolyzer capacity $\kappa_{el}$ of 500 MW and an efficiency $\eta_{el}$ of 0.72 $\mathrm{MWh_{H_2}\,MWh_{el}^{-1}}$, which is the upper limit of historically employed electrolyzer plants and produces an average of 15 261 $\mathrm{t_{Eth}\,h^{-1}}$. This yields a nominal ethylene capacity $\kappa_{Eth.}$ of 148 280 $\mathrm{t\,years^{-1}}$ which makes it comparable in capacity with low capacity steam cracking plants [32]. This is then normalized to 1 t of ethylene to match the functional unit.

Hydrogen, oxygen and $CO_2$ are the main inputs. $CO_2$ can come from various sources. Here it is assumed that $CO_2$ is captured directly from the atmosphere with a technology based on the concept used by ClimeWorks [51], which uses amine–enhanced cellulose fiber as a sorbent [52]. The energy demand can be partly met by waste heat from the process.

### *2.3. Scenario Analysis*

To asses the impact of an electrification strategy in dependence of the overall state of the energy system, we additionally analyze the development of the ESP of all technologies under two different policy scenarios for future European climate change mitigation. The **base scenario** reflects current energy policies such as taxes or subsidies but no additional climate policies. The **climate policy scenario** is based on a cumulative carbon budget of 600 Gt, compatible with meeting the more ambitious Paris target of limiting warming to 1.5°C above pre–industrial temperature with a likelihood of 67 % [1]. Table 1 gives an overview over the key characteristics of both scenarios. We use the Integrated Assessment Model REMIND to gain information on the future development of the energy supply and associated GHG and other emis-

Table 1: Employed scenarios and their main characteristics.

| | | Base | Climate Policy |
|---|---|---|---|
| **Carbon Intensity**[*] | 2020 | 0.34 | 0.28 |
| (in $t_{CO_2eq}\,MWh^{-1}$) | 2030 | 0.29 | 0.10 |
| | 2050 | 0.25 | 0.02 |
| **Carbon Price** | Implementation | No | Yes |
| (in EUR $t^{-1}_{CO_2eq}$) | 2020 | | 23.4 |
| | 2030 | | 128 |
| | 2050 | | 339 |

[*] of the European electricity grid

sions for all scenarios. Additionally, REMIND gives electricity, feedstock and carbon prices for different scenarios based on the costs of energy supply and investments necessary to reach a certain climate target, which we use for the economic analysis (see section 2.4). We start the scenario analysis at t=2015. Note that current emission levels resemble those of the climate policy scenario at t=2020 most closely. REMIND can also provide life–cycle–emissions of electricity generation until 2050, based on the methodology provided by Pehl et al. [53] and Arvesen et al. [54]. For a detailed description of REMIND see Appendix A.4.

### *2.4. Economics*

Production costs per t of ethylene give information on the economic feasibility of the different production processes. For this we use a levelized costs approach adapted from Aldersey-Williams and Rubert [55] which indicates "the minimum price at which energy [or related product] must be sold [...] to break even" [56].
Its general form is:

$$LC_{\text{Eythlene}} = \underbrace{\frac{C_\varsigma \cdot CRF + C_o}{\kappa_{Eth}}}_{\text{fixed costs}} + \underbrace{\sum_i \left(\frac{C_{ut,i}}{\eta_{ut,i}}\right)}_{\text{variable costs}} \tag{3}$$

where, $C_\varsigma$ are capital expenditures in EUR, $C_o$ are the operation and maintenance costs in EUR $\text{years}^{-1}$, $\kappa_{Eth}$ is the ethylene capacity of the plant in $t_{\text{Eth}}\,\text{years}^{-1}$, $C_{ut,i}$ are the costs of utility or feedstock i in EUR $t^{-1}$ and $\eta_{ut,i}$ is the specific utility consumption per amount of product. Revenues from by–products and electricity generation are treated as negative utility costs.
The capital recovery factor is calculated as

$$CRF = \frac{r \cdot (1+r)^a}{-1 + (1+r)^a} \tag{4}$$

Table 2: Fixed costs assumed for this study. For elektrolysis and direct air capture (DAC) we assumed capital costs to drop in the future. Year in bracket indicates the first year, where lower capital costs were assumed.

| | Steam Cracking ($\mathrm{EUR\,t^{-1}}$) | Electrolysis ($\mathrm{EUR\,kWh_{el}^{-1}}$) | DAC ($\mathrm{EUR\,t_{CO_2cap}^{-1}}$) | OCM ($\mathrm{EUR\,t_{Eth}^{-1}}$) |
|---|---|---|---|---|
| Capital costs | 1488 | 1000<br>750 (2030) | 1440<br>180 (2040) | 1274 |
| Operational costs (per year) | 76.42 | 178 | – | 63.75 |

Values are taking as average of the following reported values:
Steam Cracking: [12, 32, 57–59] for capital costs, [12, 32, 59, 60] for operational costs
OCM: Aspen Model for capital costs, operational costs are assumed to be 5 % of capital costs based on experience
Electrolyzers: [24, 61] for capital costs, [23, 62, 63] for operational costs.
Carbon Capture: [64] for capital costs, no data available for operational costs.

where $r$ is the discount factor in $\mathrm{years^{-1}}$ and $a$ is the lifetime of the plant in years. $a$ is assumed to be 30 years if not stated otherwise [55].
We deduce fixed costs for all plants from the literature except for OCM, which are estimated from the Aspen Plus model using the Aspen Process Economic Analyzer. Tab. 2 gives an overview over the capital costs assumed. For electricity, natural gas and crude oil we use prices provided from REMIND and model naphtha prices from the latter by linear regression of historical data (see Appendix A.5).
For the analysis of flexible loads, we created scenarios where electricity would only be used if prices are in the lower half or quarter of the price distribution. In return, the electrolyzer capacity and associated costs need to be doubled/quadrupled. We obtained the average electricity price of the cheapest 50 % and 25 % from present day electricity price distributions in Germany [65] as non–commercial European data is not available. As the price distribution is expected to widen with rising shares of renewables, we assume a price drop of prices in the lower half or and quartile in 2030, based on expert consultation.
Similarly we assume a price drop in capital expenditures for electrolyzers and direct air capture (DAC) in 2030 due to technological advances based on Milanzi et al. [24].

### *2.5. Tools*

All analyses are done with R run in R Studio 3.5.1 if not stated otherwise. We use Aspen Plus version 10.1 [48] to model the methanation and OCM processes. The OCM process is based on validated models previously described in Penteado et al. [39]. Appendix B provides further details of the model. Python 2.7 in Spyder 3.5.5.

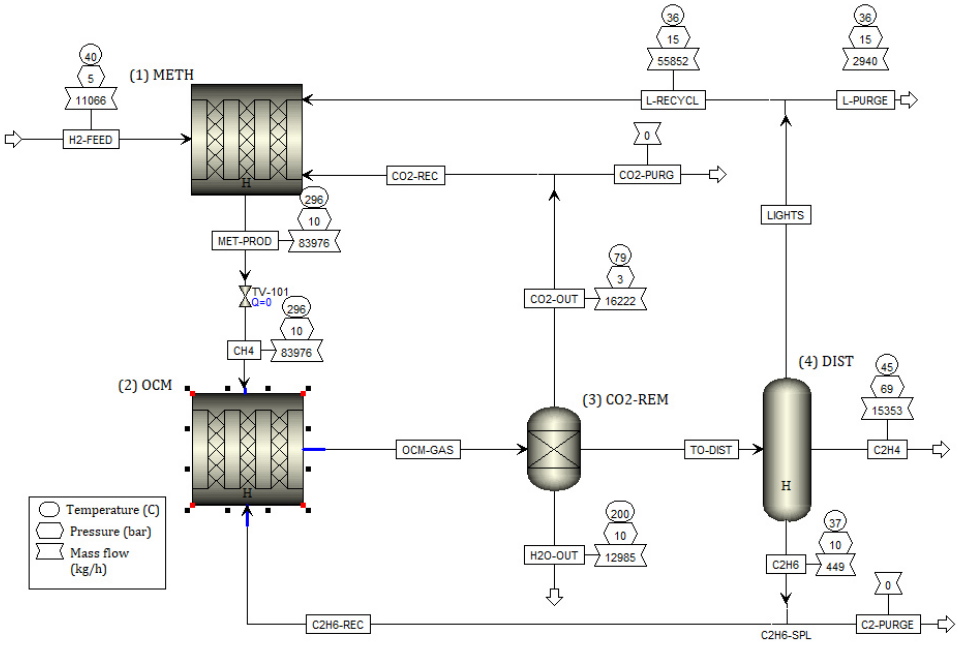


Figure 2: Simulation flowsheet of the PtG-OCM process implemented in Aspen Plus.

is used to extract emissions from the AspenPlus model, using the open source framework Bbop.

## 3. Results & Discussion

### *3.1. AspenPlus Model*

Figure 2 gives an overview of the OCM–PtG process modeled in Aspen Plus. The model consists of four main blocks: Methanation **(1)**, Oxidative Coupling of Methane **(2)**, $CO_2$ separation **(3)** and a distillation train **(4)**. It also includes two recycling loops for $CO_2$ **(CO2-REC)** and a light gas stream **(L-RECYCL)** that mainly consist of unreacted methane, but also hydrogen and carbon monoxide. Sub-flowsheets of all blocks are given in Appendix B.

The efficiency $\eta_{meth}$ of the methanation reaction is $0.83\,\mathrm{MWh_{CH_4}\,MWh_{H_2}^{-1}}$, hence the overall efficiency of the PtG system (electrolysis and methanation) is $0.6\,\mathrm{MWh_{CH_4}\,MWh_{el}^{-1}}$. These rather high efficiencies compared to the literature (e.g [17, 24]) are achieved through the internal recycling of unreacted light gases and $CO_2$. The ethylene process yield of the OCM process is $0.19\,\mathrm{t_{Eth}\,t_{CH_4}^{-1}}$. The stoichiometric yield, defined as the produced amount of ethylene divided by the stoichiometrically expected amount, would be 0.22. These findings are in agreement with values reported in the literature [50, 66], who report 0.2 and 0.24 respectively. Appendix B gives the complete stream results of the Aspen model.

### *3.2. Emissions*

Figure 3A shows emissions for cradle–to–gate as well as all cradle–to–grave systems. Cradle–to–grave emissions cluster around their EoL phase more than product type, indicating that the choice of EoL is of higher relevance for the overall emissions. As emission from polymerization are available only for PE products, the difference between different product categories might be even smaller. The relevance of EoL fate is increasing with continued electricity grid decarbonization, as emissions from recycling are reduced by continued energy system decarbonization and emission from incineration rise over time, as credits for energy exports are reduced. One functional unit of 1 t of ethylene can be used to produce multiple products, that can be either recycled or incinerated. The ribbon therefore represent the solution space of possible cradle–to–grave emissions for one functional unit.

With the current average European grid carbon intensity, indicated by the solid, vertical red lines in Figure 3, the conventional steam cracker produces between 4.88 $\mathrm{t_{CO_2eq}\,t_{Eth}^{-1}}$ to 8.88 $\mathrm{t_{CO_2eq}\,t_{Eth}^{-1}}$. The electrified steam cracker produces between 7.17 a to 10.17 and the OCM–PtG process between 13.82 $\mathrm{t_{CO_2eq}\,t_{Eth}^{-1}}$ to 15.76 $\mathrm{t_{CO_2eq}\,t_{Eth}^{-1}}$. Through a complete decarbonization of the electricity supply, emissions from the conventional steam cracker are reduced to between 4.29 $\mathrm{t_{CO_2eq}\,t_{Eth}^{-1}}$ to 8.01 $\mathrm{t_{CO_2eq}\,t_{Eth}^{-1}}$, from the electrified steam cracker to between 4.29 $\mathrm{t_{CO_2eq}\,t_{Eth}^{-1}}$ to 8.01 $\mathrm{t_{CO_2eq}\,t_{Eth}^{-1}}$ and from OCM–PtG to between −2.57 $\mathrm{t_{CO_2eq}\,t_{Eth}^{-1}}$ to 1.14 $\mathrm{t_{CO_2eq}\,t_{Eth}^{-1}}$.

This already shows that while it is possible to achieve a carbon neutral or net–negative production pathway with OCM–PtG, the sign of the net emission flow cannot be predicted without detailed knowledge of the EoL fate. With complete incineration, a net–negative production is not possible and the required share of recycling depends on the carbon intensity of electricity. Figure 3 also shows that it requires an electricity carbon intensity of less than 0.08 $\mathrm{t_{CO_2eq}\,MWh^{-1}}$ to achieve a carbon neutral process.

Figure 3B and C give the absolute and relative ESP, where filled symbols represent the standard product systems. The electrified steam cracker yields an ESP of −1.29 $\mathrm{t_{CO_2eq}\,t_{Eth}^{-1}}$, which rises to 0 $\mathrm{t_{CO_2eq}\,t_{Eth}^{-1}}$ through a complete decarbonization. Therefore, while overall emissions are reduced, the process at no point in time has a positive ESP, i.e. a lower emissions production than the conventional process.

In the case of OCM–PtG, the ESP ranges from −7.94 $\mathrm{t_{CO_2eq}\,t_{Eth}^{-1}}$ to 6.87 $\mathrm{t_{CO_2eq}\,t_{Eth}^{-1}}$. Therefore, the conventional process is currently still the best option, but after a complete grid decarbonization, OCM–PtG becomes favorable in terms of emissions. The relative ESP of OCM–PtG ranges from −2, i.e. an almost three–fold increase in emissions, under present conditions to 2 with a completely decarbonized electricity grid, wherein OCM–PtG reduces the emissions of conventional steam cracking by three–fold.

In the following, the emissions profiles of all product systems are discussed in more detail. Figure 4 show energy and carbon flows for all product systems and Figure 5A provides detailed disaggregated emission profiles.

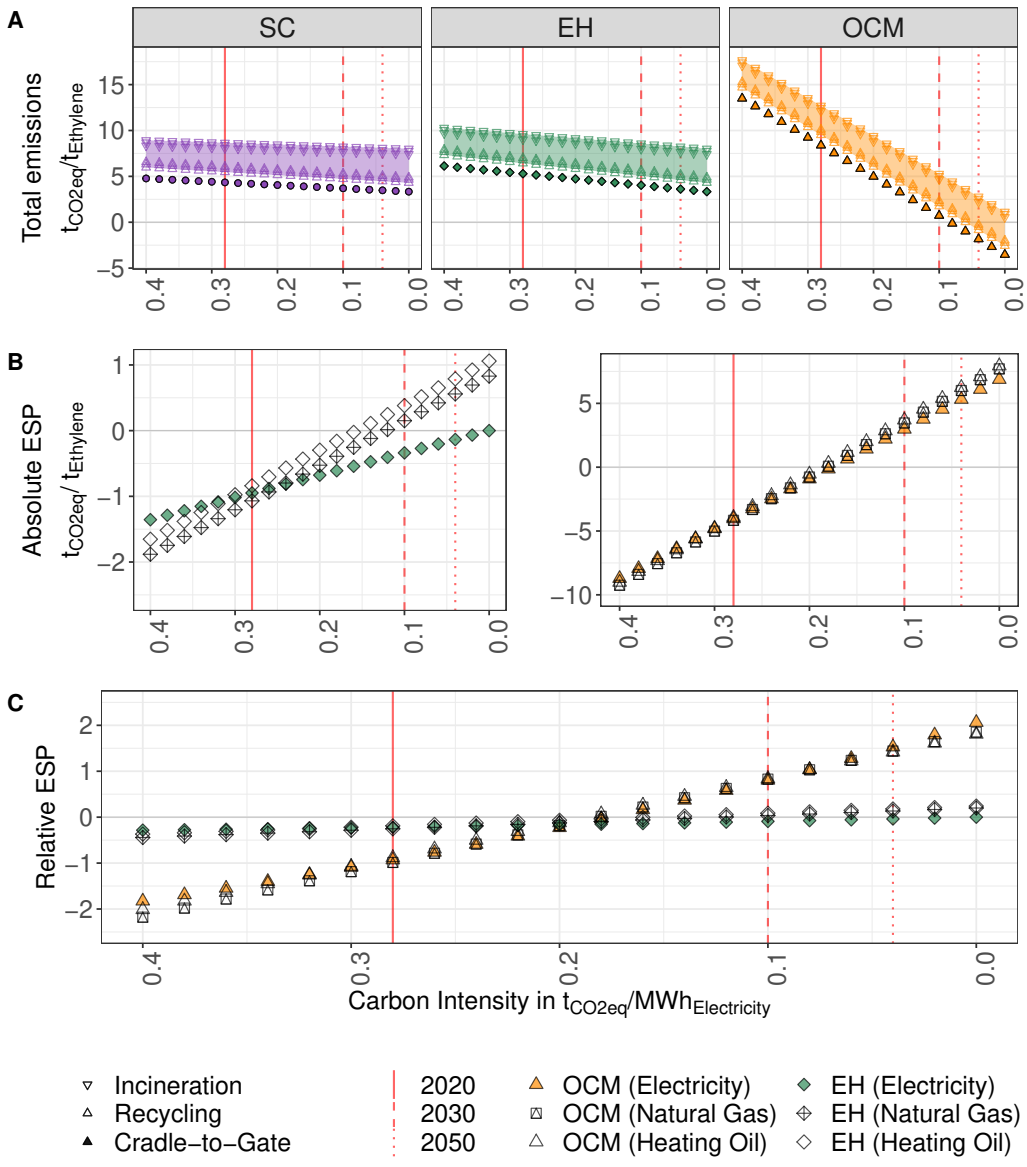


Figure 3: Emissions of all product systems dependent on carbon intensity of electricity. Red lines indicate when these conditions will be reached in the investigated 1.5°C scenario. **A**: Total emissions for cradle–to–gate and different end–of–life strategies. **B**: Absolute emission saving potential of all alternative configurations compared to the conventional steam cracker. A negative ESP indicates a disadvantageous process configuration, a positive ESP indicates an improvement. Note that range of y-axes differs. **C**: Relative ESP fo the same configurations

*3.2.1. Electrified Steam Cracker*

Under current grid carbon intensities, the electrified steam cracker produces slightly higher emissions than the conventional one. While the total emissions of both configurations are reduced by around 30 % through a complete grid decarbonization, the minimal emissions achievable are identical for both systems. The electrified steam cracker therefore never results in reduced emissions compared to the conventional process.

While this finding seems curious as first, the flow diagrams in Figure 4B and disaggregated emissions, shown in Figure 5A, explain why this is the case. The bulk of emissions in steam cracking stems from upstream naphtha refinery ($1.91\,\mathrm{t_{CO_2eq}\,t_{Eth}^{-1}}$) and the combustion of off–gases ($1.42\,\mathrm{t_{CO_2eq}\,t_{Eth}^{-1}}$), either for process heating or downstream. As the general structure of the process remains unaffected through electrification, the same amount of fossil carbon is introduced to the process via naphtha, producing the same amount of upstream emissions, products and high–energetic gases. It is very likely that these gases will be valorized at some point along their value chain. Here, we assume they are combusted in a gas–fired power plant. Therefore, the emissions originating from off–gas combustion are shifted down the value chain rather than eliminated. Note that other uses are possible and are discussed in section 3.2.3.

We would also like to note, that in our case we assumed steam cracking to be entirely fueled by off-gases. However, this might not be true for all existing Naphtha steam crackers. If an external fuel source is supplied, electric steam cracking might yield some emissions reductions. Since Naphtha cracking usually provides a large fraction of its energy demand by off-gases, we expected this effect to be in any case small [32].

The remaining emissions stem from electricity, which are affected by grid decarbonization, and which are larger in the case of electrification. This can be explained by the fact that the additional amount of electricity supplied to the electrified steam cracker needs to equal the lower heating value (LHV) of the off–gases fed to the furnace otherwise (assuming constant furnace efficiency), while the additional amount of electricity provided to the conventional steam cracker as system expansion needs to equal the amount of electricity generated from the off–gases in the electrified version, which is less. Put differently, the transformation of elementary inflows to functional unit includes an additional conversion step in the electrified version, reducing the overall system efficiency.

*3.2.2. OCM–PtG*

Figure 4C shows that the process structure of OCM–PtG is fundamentally different from that of steam cracking, as the main energy source (hydrogen) is separated from the carbon source ($CO_2$). It also becomes clear that under present conditions, emissions from OCM–PtG are more than twice the emissions from the conventional steam cracker. Figure 5A also provides disaggregated emissions for OCM–PtG. The

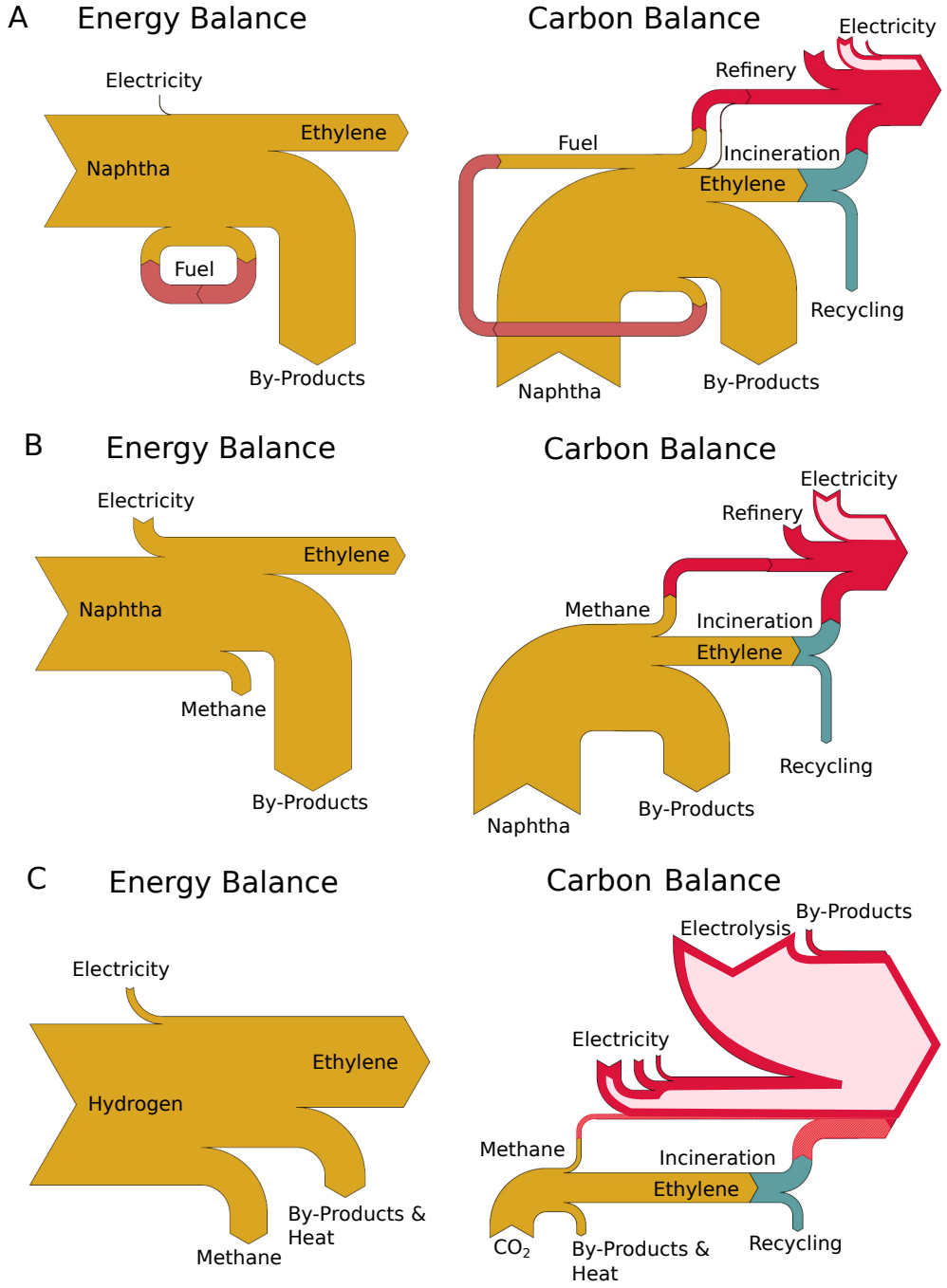


Figure 4: Energy and carbon flows for **A**: Conventional Steam Cracking **B**: Electrified Steam Cracking and **C**: OCM-PtG. Yellow represents main process, green represents EoL, red represents carbon from $CO_2$. Carbon intensity is $0.4\,t_{CO_2eq}\,MWh^{-1}$, light red shows associated carbon flows eliminated through decarbonization. Hatched red indicates captured carbon. EoL strategy ratio is arbitrary chosen for illustration.

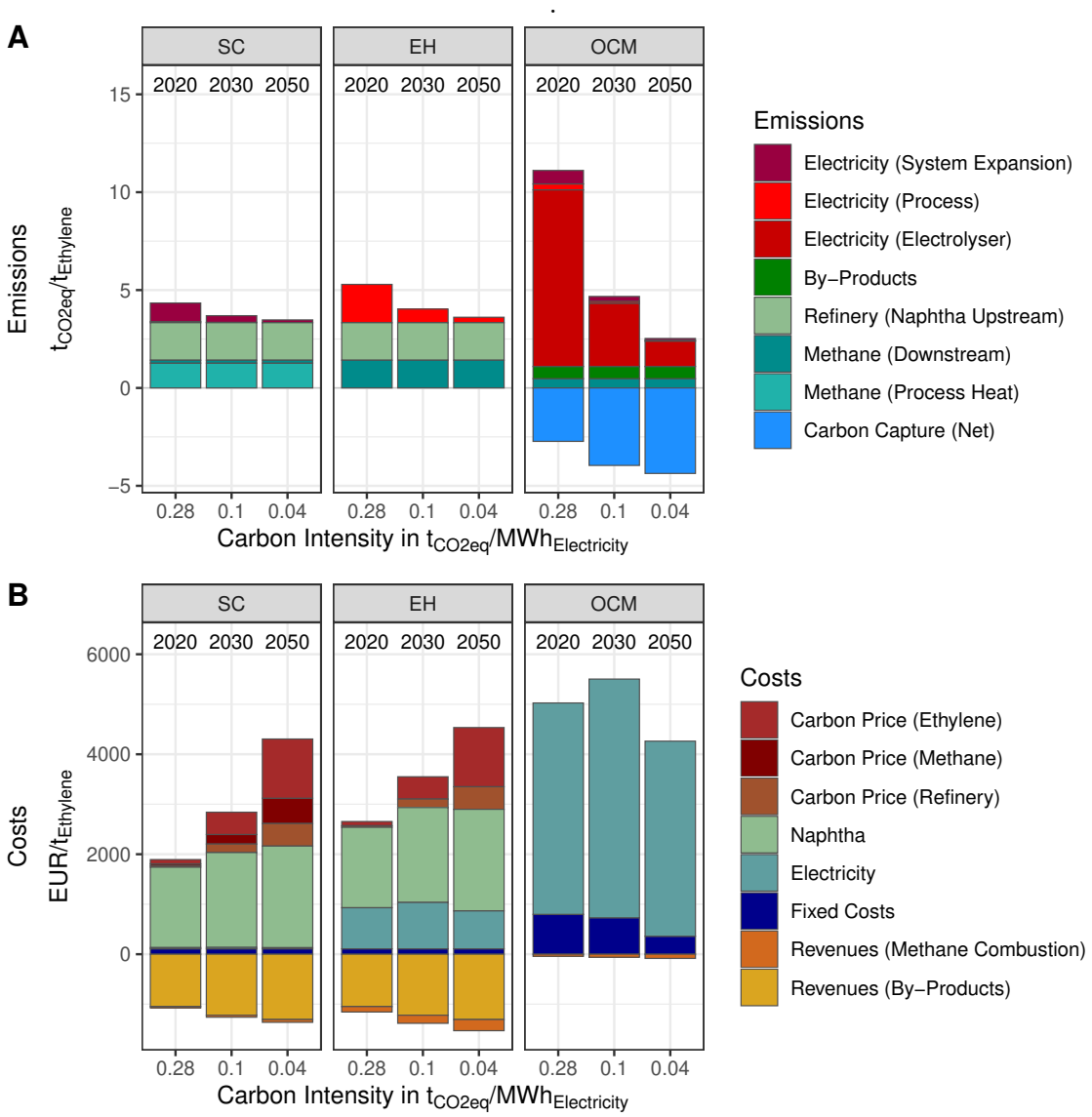


Figure 5: **A**: Disaggregated emission profile of main process configurations. **B**: Disaggregated cost profiles of main process configurations. For each process we show the configuration whose grid carbon intensities and carbon prices correspond to the timesteps 2020, 2030 and 2050 in the investigated climate policy scenario.

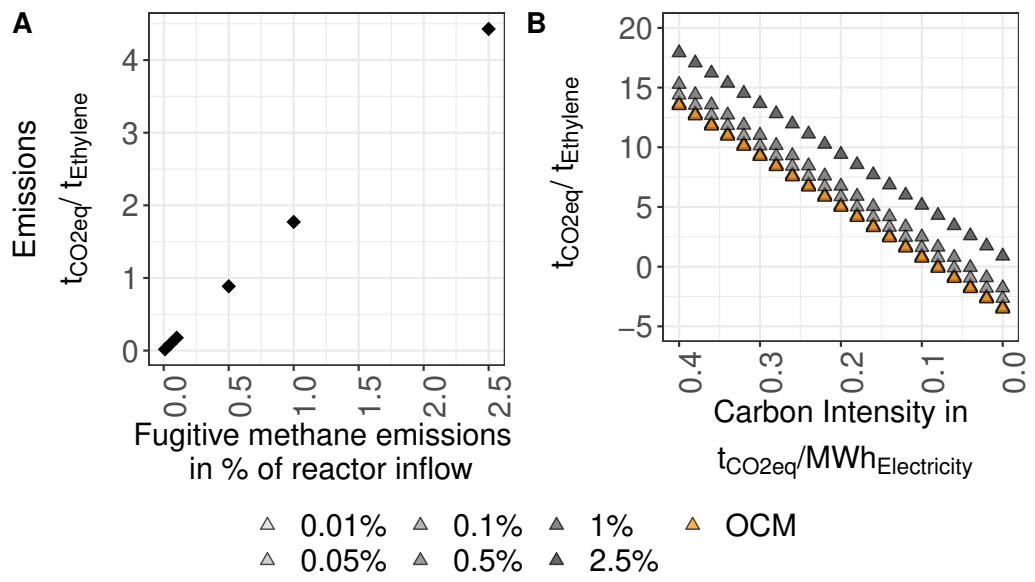


Figure 6: **A**: Different amounts of fugitive methane emissions, modeled as shares of the reactor inflow and represented as $CO_2$ equivalents. **B**: Effect of fugitive methane emissions on the cradle–to–gate emissions of OCM–PtG.

main contributor is the hydrogen production via electrolysis ($12.2\,\mathrm{t_{CO_2eq}\,t_{Eth}^{-1}}$), with minor contributions from other electricity, off–gas combustion and system expansion. Emissions from carbon capture are $-2.05\,\mathrm{t_{CO_2eq}\,t_{Eth}^{-1}}$, which represents the net of the negative emission flow of captured carbon and the positive emissions flow of the energy needed to accomplish this.

Since the majority of OCM–PtG emissions stem from electricity, grid decarbonization has a profound effect on reducing emissions. Emissions associated with the electrolysis are reduced to $1.29\,\mathrm{t_{CO_2eq}\,t_{Eth}^{-1}}$ through grid decarbonization. Additionally $0.14\,\mathrm{t_{CO_2eq}\,t_{Eth}^{-1}}$ from other electricity sources remain and $1.10\,\mathrm{t_{CO_2eq}\,t_{Eth}^{-1}}$ of non–electric emissions that are unaffected by grid decarbonization. The magnitude of the net negative emissions from carbon capture also increases to $-4.37\,\mathrm{t_{CO_2eq}\,t_{Eth}^{-1}}$ through a decarbonization of its energy supply, enhancing the overall reduction effect even further.

However, a major source of uncertainty is the amount of FME released during the process. Figure 6 shows the effect of FME on process performance. An assumed leakage of 2.5 % of the reactor inflow would lead to additional emissions of 4.42 $\mathrm{t_{CO_2eq}\,t_{Eth}^{-1}}$, reducing the ESP of OCM–PtG by 30 %. Even a leakage of 0.5 % would result in additional emissions of $0.89\,\mathrm{t_{CO_2eq}\,t_{Eth}^{-1}}$. It is therefore of high relevance to gain more experimental data and establish estimation methodologies regarding the amounts of methane leakages from power–to–gas plants if they continue to gain traction as a key technology in energy systems transformation.

*3.2.3. The role of system expansion*

The results above, however, depend on the system expansion chosen. While we think it valid to assume that off–gases will be valorized and that this most likely will include their combustion, other uses than electricity generation are possible. Figure 3B and C also give the ESP for the two other product systems, where off–gases either substitute natural gas or residual heating oil (unfilled symbols). In the case of electrified steam cracking neither system yields a positive ESP under present conditions while the two alternative systems have the potential to do so once the electricity supply is sufficiently decarbonized. The heating oil system yields a maximal ESP of $1.05\,\mathrm{t_{CO_2eq}\,t_{Eth}^{-1}}$ and the natural gas system a slightly lower of $0.83\,\mathrm{t_{CO_2eq}\,t_{Eth}^{-1}}$. Electrification of steam cracking can therefore result in a net emission saving, if the off–gases produce a service, whose alternative realization is more carbon intensive then the grid electricity used in the electric furnace. OCM–PtG shows a slightly different effect, as all three product systems yield positive ESPs for low carbon intensities. Here, however the differences between the three product systems are of less relevance compared to the overall magnitude of the ESP and the effect of decarbonization.

*3.3. Scenario Analysis*

We next analyzed how the proposed reductions in grid carbon intensity play out in an economy–wide decarbonization scenario to gain information on the expected time frames and costs.

*3.3.1. Emissions*

Figure 7A shows the development of cradle–to–grave emissions under the two analyzed scenarios until 2050. In the base scenario, i.e. without additional climate policies, the critical decarbonization, upon which the emissions from OCM–PtG fall below those of steam cracking, is not reached. In the climate policy scenario, a grid decarbonization, where OCM–PtG produces less emissions than steam cracking independently of the end–of–life strategy, is realized in 2030, i.e. at a carbon intensity of $0.1\,\mathrm{t_{CO_2eq}\,MWh^{-1}}$. A net–negative process, assuming 100 % recycling, can first be realized in 2030, at a carbon intensity of $0.08\,\mathrm{t_{CO_2eq}\,MWh^{-1}}$. After complete decarbonization, the values stay clustered around zero. Therefore, detailed information on the product EoL fate is always required to properly determine if a net zero emission flow can actually be achieved.

*3.3.2. Economics*

Figure 7B gives the obtained levelized costs of ethylene production for all product systems. Additionally, Figure 5B gives disaggregated costs for chosen time steps. Costs from the conventional steam cracker start at around $650.4\,\mathrm{EUR\,t_{Eth}^{-1}}$ and rise to $1144\,\mathrm{EUR\,t_{Eth}^{-1}}$ in the base scenario and $2942\,\mathrm{EUR\,t_{Eth}^{-1}}$ in the climate policy scenario. For the electrified steam cracker costs start at $1400\,\mathrm{EUR\,t_{Eth}^{-1}}$ and rise to

$1743\,\mathrm{EUR\,t_{Eth}^{-1}}$ in the base and $3004\,\mathrm{EUR\,t_{Eth}^{-1}}$ in the climate policy scenario. The reason for the rising costs are a rise in naphtha prices, the main cost element, as the used Integrated Assessment Model REMIND expects fossil resources to become gradually depleted over time. In the case of policy scenarios, an additional carbon price is implemented on any fossil carbon introduced into the economy (see table 1). In the case of OCM–PtG no clear difference in cost development is visible in the implemented scenarios with costs varying between $4000\,\mathrm{EUR\,t_{Eth}^{-1}}$ and $5000\,\mathrm{EUR\,t_{Eth}^{-1}}$, exhibiting minor cost reductions through technological learning in both. Electricity dominates costs of OCM–PtG, followed by capital expenditures for the electrolyzer and the DAC unit. It is clear from Figure 7B that OCM–PtG is not cost–competitive in any scenario.

Figure 7B also shows the potential cost reductions from a flexible electrolyzer load regime (unfilled symbols). While under present conditions the costs of the different load regimes are at par, flexible loads are able to bring down the overall costs as soon as a large–scale employment of renewable energy broadens the electricity price distribution. Consequently, the effect is more profound in the climate policy scenario scenario, where OCM–PtG breaks even around the year 2040. While these results show the general potential of flexible loads to bring down costs, the price distributions assumed here are only rough estimates and so are the derived results. In–depth analyses of the future expected electricity price spread and its economic implications are necessary for a more precise estimation.

In sum, the economic analyses show that making OCM–PtG cost–competitive is challenging. The main factors that control the cost differences are the development of feedstock (naphtha) and electricity prices and the capital expenditures of the electrolyzer and DAC units.

## 4. Conclusion

We show that under the current European electricity grid carbon intensity, neither direct nor indirect electrification result in a net reduction of ethylene production emissions. However, both strategies have the potential to do so, albeit to varying degrees and highly dependent on external parameters. In the case of direct electrification, the emission saving potential compared to conventional steam cracking is $-1.74\,\mathrm{t_{CO_2eq}\,t_{Eth}^{-1}}$ to $0.95\,\mathrm{t_{CO_2eq}\,t_{Eth}^{-1}}$ depending on the electricity source and the fate of co–produced high–energetic off–gases. The emission saving potential of OCM–PtG ranges from $-8.54\,\mathrm{t_{CO_2eq}\,t_{Eth}^{-1}}$ to $6.52\,\mathrm{t_{CO_2eq}\,t_{Eth}^{-1}}$, highly depended on the electricity source, i.e. carbon intensity, and to a lesser extend on off–gas fate. The highest ESP is reached if a decarbonized electricity source is used and off–gases substitute emission–intensive fossil fuels such as residential heating oil.

Direct electrification of steam cracking alone can not bring emissions to a level that is compatible with a zero–carbon economy due to the residual emissions from oil refining and the energetic utilization of fossil–based by–products, that make up 70 % of the

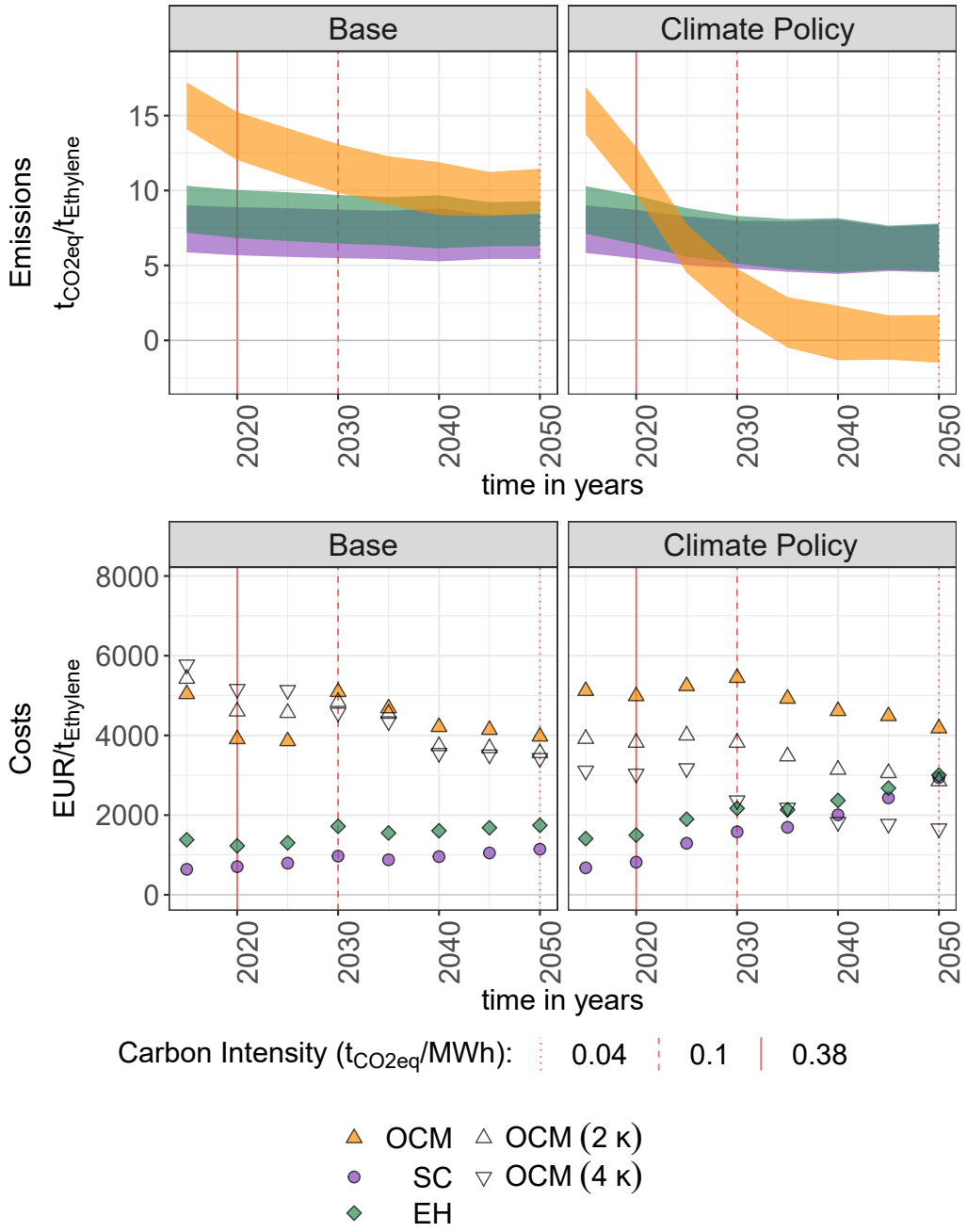


Figure 7: Scenario data for base and climate policy scenario **A**: Cradle–to–grave emissions range for all three product systems. **B**: Levelized costs of the different main product systems, indicating the minimal price at which ethylene needs to be sold to break even. Unfilled symbols show effect of electrolyzer flexibilisation on the levelized costs of ethylene produced by OCM–PtG. $2\kappa$ doubles electrolyzer capacity and halfs load hours, $4\kappa$ quadruples electrolyzer capacity and quarters load hours.

overall emissions. OCM–PtG on the other hand can achieve zero–net emissions over its life cycle, as it completely substitutes the fossil carbon input through atmospheric carbon and a carbon-free energy source. While an electricity grid carbon intensity of $0.1\,\mathrm{t_{CO_2eq}\,MWh^{-1}}$ is the minimal requirement for OCM–PtG to yield a positive ESP, a minimal carbon intensity of $0.08\,\mathrm{t_{CO_2eq}\,MWh^{-1}}$ is necessary to achieve a zero–net process. However, the definite sign of the net emission flow depends on the end–of–life fate. A certain share of recycling will always be necessary to achieve net–negative emissions over the life cycle.

Our scenario analysis shows that even under a stringent climate policy compatible with the Paris target of a 1.5°C temperature limit, the conditions ensuring a beneficial effect or a net–zero process from OCM–PtG based on grid carbon intensity will no be achieved before 2030 and 2035 respectively. However, the scenarios give only European averages. In a specific case, necessary grid carbon intensities might be realized earlier or later.

In this context is important to note that none of the external parameters relevant to life–cycle emissions are usually under the control of an ethylene or polymer producer. Additionally the economic analysis shows that the cost–competitiveness of OCM–PtG is difficult to achieve in the near and mid–term future. Any entity promoting electrification as a mitigation strategy worth of additional financial support must therefore find an answer on how to ensure the necessary electricity carbon intensity, off–gas substitution and recycling rate.

Furthermore, our results provide some general insights into the nature of emissions from petrochemical processes and ways to reduce them. Fossil fuels have a double role in the petrochemical industry as being both fuel and raw material with the two purposes often inextricable linked. Electrification of the process has therefore limited influence on the overall energy and carbon flows, as the feedstock provides both the main energy and the main carbon input. As the chemical equilibrium of any oxidation of hydrocarbons strongly favours the formation of $CO_2$, it is almost unavoidable that a certain fraction of that feedstock will be utilized energetically somewhere along the value chain.

This view can also be extended to plastic products. Plastics are the waste stream with the highest calorific value [67, 68], which in general makes their energetic recovery (incineration) an attractive and likely EoL strategy. Therefore, a zero–emissions transformation of the polymer and plastics industry does not stop at production processes but needs to take into account the whole life cycle of the product.

Therefore, next to detailed analyses of additional low–carbon production pathways such as the methanol–to–olefins route or biomass–based processes, strategies for waste recycling and reduction need to be considered as well when developing the overall best strategy. While a certain amount of CCU can be advantageous for closing the industrial carbon cycle and achieving a net–zero–emission scenario, the associated energy costs of $CO_2$ fixation are high and can also counteract mitigation efforts. Material and monomer recycling options such as pyrolysis or gasification

are less energy intensive and might be advantageous in many applications. They should therefore receive more attention in the debate. Additional environmental impact categories as reflected in a full life cycle analysis might also be helpful to complete the picture [69]. In this context we would also like to note that current and projected plastic consumption patterns are likely not to be rendered sustainable with any production process available. Therefore, demand side solutions such as less material-intensive lifestyles and greater material efficiencies in product services are important mitigation options and should be central to a holistic industry decarbonization strategy.

**Author contributions:** L.S.L., I. D., G. L., A. T. P. and F.U. conceptualized the study. A. T. P. designed and validated the AspenPlus model. L.S.L conducted the simulations and performed the analyses, all authors interpreted the results. L. S. L. wrote the manuscript with contributions from all authors. All authors have read and agreed to the published version of the manuscript.

**Data accessibility:** Data and code for this paper are available at `https://github.com/lucialenasophie/ethylene_decarbonisation`. The open source framework Bbop for the Python-Aspen connectivity is available at `gitlab.tubit.tu-berlin.de/dbta/bbop.git`.

**Acknowledgements:** The authors thank Michaja Pehl for provision of the life cycle coefficients for REMIND as well as Alois Dirnaichner, David Klein and Silvia Madeddu for valuable help and discussions. This work was partially funded by the START project from the German Federal Ministry of Education and Research (BMBF, 03EK3046A) and by the Volkswagen Sustainability Council. L. S. L. is additionally grateful for financial support from the Friedrich Ebert Foundation. A. T. P. gratefully acknowledges financial support from the German Federal Ministry of Education and Research (BMBF 01DN17023) and CAPES/ Brazil (11946/13-0)

**Conflict of interest:** The authors declare no conflict of interest.

**List of abbreviations**

**Acronyms**

**CCU** carbon capture and utilization

**DAC** direct air capture

**EoL** end–of–life

**ESP** emission saving potential

**FME** fugitive methane emissions

**GHG** greenhouse gas

**HVCs** high value chemicals

**IPCC** Intergovermental Panel on Climate Change

**LHV** lower heating value

**OCM** Oxidative Coupling of Methane

**PE** polyethylene

**PtG** Power–to–Gas

**PVC** polyvinylchloride

**SC** Steam cracking

**t** metric ton

## References


[1] Masson-Delmotte, V., P., Z., H.-O, P., D., R., J., S., P.R., S., et al. Global Warming of 1.5 degree celsius. An IPCC Special Report on the impacts of global warming of 1.5 degree celsius above pre-industrial levels and related global greenhouse gas emission pathways, in the context of strengthening the global response to the threat of climate change, sustainable development, and efforts to eradicate poverty. Special report; [Geneva, Switzerland]: IPCC; 2018. ISBN 978-92-9169-151-7.

[2] Luderer, G., Vrontisi, Z., Bertram, C., Edelenbosch, O.Y., Pietzcker, R.C., Rogelj, J., et al. Residual fossil $CO_2$ emissions in 1.5–2 °C pathways. Nature Climate Change 2018;8(7):626–633. doi:\bibinfo{doi}{10.1038/s41558-018-0198-6}.

[3] Posen, I.D., Jaramillo, P., Landis, A.E., Griffin, W.M.. Greenhouse gas mitigation for U.S. plastics production: Energy first, feedstocks later. Environmental Research Letters 2017;12(3):034024. doi:\bibinfo{doi}{10.1088/1748-9326/aa60a7}.

[4] Åhman, M., Nilsson, L.J., Johansson, B.. Global climate policy and deep decarbonization of energy-intensive industries. Climate Policy 2016;17(5):634–649. doi:\bibinfo{doi}{10.1080/14693062.2016.1167009}.

[5] European Comission, . A roadmap for moving to a competitive low carbon economy in 2050 /* COM/2011/0112 final */: Document 52011DC0112. 2011. URL https://eur-lex.europa.eu/legal-content/EN/ALL/?uri=CELEX%3A52011DC0112.

[6] BMUB (Federal Ministry for the Environment, Nature Conservation, Building and Nuclear Safety), . Climate action plan 2050: Principles and goals of the german government's climate policy. 2016.

[7] Davis, S.J., Lewis, N.S., Shaner, M., Aggarwal, S., Arent, D., Azevedo, I.L., et al. Net-zero emissions energy systems. Science (New York, NY) 2018;360(6396). doi:\bibinfo{doi}{10.1126/science.aas9793}.

[8] Schiffer, Z.J., Manthiram, K.. Electrification and decarbonization of the chemical industry. Joule 2017;1(1):10–14. doi:\bibinfo{doi}{10.1016/j.joule.2017.07.008}.

[9] Lechtenböhmer, S., Nilsson, L.J., Åhman, M., Schneider, C.. Decarbonising the energy intensive basic materials industry through electrification – implications for future EU electricity demand. Energy 2016;115:1623–1631. doi:\bibinfo{doi}{10.1016/j.energy.2016.07.110}.

[10] Bühler, F., Zühlsdorf, B., Nguyen, T.V., Elmegaard, B.. A comparative assessment of electrification strategies for industrial sites: Case of milk powder production. Applied Energy 2019;250:1383 – 1401.

[11] Ren, T., Patel, M., Blok, K.. Olefins from conventional and heavy feedstocks: Energy use in steam cracking and alternative processes. Energy 2006;31(4):425–451. doi:\bibinfo{doi}{10.1016/j.energy.2005.04.001}.

[12] International Energy Agency, . Energy and GHG reductions in the chemical industry via catalytic processes. 2013.

[13] Brightlands, . Petrochemical companies form cracker of the future consortium and sign r & d agreement. 2019. URL https://www.brightlands.com/en/brightlands-chemelot-campus/news/petrochemical-companies-form-cracker-future-consortium-and-sign-rd.

[14] ICIS, . BASF aims to develop electric furnaces for steam cracking to cut $CO_2$ emissions. 2019. URL https://www.icis.com/explore/resources/news/2019/01/10/10304937/basf-aims-to-develop-electric-furnaces-for-steam-cracking-to-cut-co2-emissions/.

[15] van Delft, Y., Kler, , Remco, . Matching processes with electrification technologies. 2016.

[16] Sterner, M.. Bioenergy and renewable power methane in integrated 100% renewable energy systems. Kassel University Press; 2009. ISBN 9783899587982.

[17] Götz, M., Lefebvre, J., Mörs, F., McDaniel Koch, A., Graf, F., Bajohr, S., et al. Renewable power-to-gas: A technological and economic review. Renewable Energy 2016;85:1371–1390. doi:\bibinfo{doi}{10.1016/j.renene.2015.07.066}.

[18] Buchholz, O.S., van der Ham, A., Veneman, R., Brilman, D., Kersten, S.. Power-to-gas: Storing surplus electrical energy. a design study. Energy Procedia 2014;63:7993–8009. doi:\bibinfo{doi}{10.1016/j.egypro.2014.11.836}.

[19] Bazzanella, A., Ausfelder, F.. Low carbon energy and feedstock for the european chemical industry. 2017.

[20] Rissman, J., Bataille, C., Masanet, E., Aden, N., Morrow, W.R., Zhou, N., et al. Technologies and policies to decarbonize global industry: Review and assessment of mitigation drivers through 2070. Applied Energy 2020;266. doi:\bibinfo{doi}{10.1016/j.apenergy.2020.114848}.

[21] Sternberg, A., Bardow, A.. Power-to-what? – environmental assessment of energy storage systems. Energy & Environmental Science 2015;8(2):389–400. doi:\bibinfo{doi}{10.1039/C4EE03051F}.

[22] Lehner, M.. Power-to-Gas: Technology and business models. Springer briefs in energy; Cham and Heidelberg: Springer; 2014. ISBN 978-3-319-03995-4.

[23] Berliner Abfall-und Energiekonferenz, , editor. Integration einer Power-to-Methan Anlage mit $CO_2$-Abscheidung aus dem Abgas in der Kehrichtverbrennungsanlage Lint [Integration of a Power-to-Gas-Process with $CO_2$-Capture of the Waste-to-Energy-Plant Linth]. 2019.

[24] Milanzi, S., Spiller, C., Grosse, B., Hermann, L., Kochems, J., Müller-Kirchenbauer, J.. Technischer Stand und Flexibilität des Power-to-Gas-Verfahrens german [Technical status and flexibility of Power-to-Gas-Processes]. 2018.

[25] Giglio, E., Deorsola, F.A., Gruber, M., Harth, S.R., Morosanu, E.A., Trimis, D., et al. Power-to-gas through high temperature electrolysis and carbon dioxide methanation: Reactor design and process modeling. Industrial & Engineering Chemistry Research 2018;57(11):4007–4018. doi:\bibinfo{doi}{10.1021/acs.iecr.8b00477}.

[26] Hauke, H., Emele, Lukas, Loreck, Charlotte, . Pruefung der klimapolitischen konsistenz und der kosten von methanisierungsstrategien [assessment of political coherence and costs of methanation strategies]. 2014.

[27] Mac Dowell, N., Fennell, P.S., Shah, N., Maitland, G.C.. The role of $CO_2$ capture and utilization in mitigating climate change. Nature Climate Change 2017;7(4):243–249. doi:\bibinfo{doi}{10.1038/nclimate3231}.

[28] Bals, C., Bellmann, E., Bode, A., Edenhofer, O., Fischedick, M., Gaertner, L.E., et al. CCU and CCS – building blocks for climate protection in industry. 2018.

[29] European Comission, . Novel carbon capture and utilization technologies. 2018.

[30] von der Assen, N., Bardow, A.. Life cycle assessment of polyols for polyurethane production using $CO_2$ as feedstock: Insights from an industrial case study. Green Chemistry 2014;16(6):3272–3280. doi:\bibinfo{doi}{10.1039/C4GC00513A}.

[31] Meys, R., Kätelhön, A., Bardow, A.. Towards sustainable elastomers from $CO_2$: Life cycle assessment of carbon capture and utilization for rubbers. Green Chemistry 2019;21(12):3334–3342. doi:\bibinfo{doi}{10.1039/C9GC00267G}.

[32] Zimmermann, H., Walzl, R.. Ethylene. in Ullmann's Encyclopedia of Industrial Chemistry. Wiley; 2000. ISBN 9783527303854. doi:\bibinfo{doi}{10.1002/14356007}.

[33] Kaetelhoen, A., Meys, R., Deutz, S., Suh, S., Bardow, A.. Climate change mitigation potential of carbon capture and utilization in the chemical industry. Proceedings of the National Academy of Sciences of the United States of America 2019;116(23):11187–11194. doi:\bibinfo{doi}{10.1073/pnas.1821029116}.

[34] Palm, E., Nilsson, L.J., Åhman, M.. Electricity-based plastics and their potential demand for electricity and carbon dioxide. Journal of Cleaner Production 2016;129:548–555. doi:\bibinfo{doi}{10.1016/j.jclepro.2016.03.158}.

[35] Keller, G., Bhasin, M.. Synthesis of ethylene via oxidative coupling of methane i. determination of active catalysts. Journal of Catalysis 1982;73(1):9–19. doi:\bibinfo{doi}{10.1016/0021-9517(82)90075-6}.

[36] Degnan, T.. Siluria and OCM – close to full scale commercializaton? Focus on Catalysts 2016;2016:1–2. doi:\bibinfo{doi}{10.1016/j.focat.2016.11.001}.

[37] Jernigan, B.. Siluria technologies and saudi aramco technologies company join forces to maximize chemicals production. 2018. URL `https://siluria.com/Newsroom/Press_Releases`.

[38] Stangland, E.E.. The shale gas revolution: A methane-to-organic chemicals renaissance? In: Frontiers in Engineering: Reports on Leading-Edge Engineering from the 2014 Symposium. 2014,.

[39] Penteado, A.T., Kim, M., Godini, H.R., Esche, E., Repke, J.U.. Techno-economic evaluation of a biogas-based oxidative coupling of methane process for ethylene production. Frontiers of Chemical Science and Engineering 2018;12(4):598–618. doi:\bibinfo{doi}{10.1007/s11705-018-1752-5}.

[40] ISO, . ISO 14040:2006 - environmental management - life cycle assesment - principles and framework. 2006.

[41] ISO, . ISO 14044:2006 - environmental management - life cycle assessment - requirements and guidelines. 2006.

[42] ISO, . ISO 14067:2018 - greenhouse gases – carbon footprint of products – requirements and guidelines for quantification. 2018.

[43] Eggleston, H.S.. 2006 IPCC guidelines for national greenhouse gas inventories. Hayama, Japan: Institute for Global Environmental Strategies; 2006. ISBN 4-88788-032-4.

[44] Zhou, X., Passow, F.H., Rudek, J., von Fisher, J.C., Hamburg, S.P., Albertson, J.D.. Estimation of methane emissions from the U.S. ammonia fertilizer industry using a mobile sensing approach. Elem Sci Anth 2019;7(1):19. doi:\bibinfo{doi}{10.1525/elementa.358}.

[45] thinkstep, . GaBi LCA professional database. 2019.

[46] Stocker, T., editor. Climate change 2013: The physical science basis: Working Group I contribution to the fifth assessment report of the Intergovernmental Panel on Climate Change. Cambridge: Cambridge University Press; 2014. ISBN 9781107661820. doi:\bibinfo{doi}{10.1017/CBO9781107415324}. URL `https://doi.org/10.1017/CBO9781107415324`.

[47] de Bruijn, H., van Duin, R., Huijbregts, M.A.J.. Handbook on Life Cycle Assessment; vol. 7 of *Eco-Efficiency in Industry and Science*. Dordrecht: Springer Netherlands; 2002. ISBN 978-1-4020-0228-1 978-0-306-48055-3. doi:\bibinfo{doi}{10.1007/0-306-48055-7}. URL `http://link.springer.com/10.1007/0-306-48055-7`.

[48] Aspen Technology Inc., . Aspenplus. 2019.

[49] Peng, D.Y., Robinson, D.B.. A new two-constant equation of state. Industrial & Engineering Chemistry Fundamentals 1976;15(1):59–64. doi:\bibinfo{doi}{10.1021/i160057a011}.

[50] Friedel, M., Nitzsche, J., Krause, H.. Katalysatorscreening und Reaktormodellierung für die oxidative Methankopplung zur Brennwertanhebung von Biogas [catalyst screening and reactor modelling for increasing the heating

value of biogas via oxidative coupling of methane]. Chemie Ingenieur Technik 2017;89(6):715–723. doi:\bibinfo{doi}{10.1002/cite.201600018}.

[51] ClimeWorks, . Direct air capture & storage (DACS) factsheet for researchers. 2019.

[52] Fasihi, M., Efimova, O., Breyer, C.. Techno-economic assessment of $CO_2$ direct air capture plants. Journal of Cleaner Production 2019;224:957–980. doi:\bibinfo{doi}{10.1016/j.jclepro.2019.03.086}.

[53] Pehl, M., Arvesen, A., Humpenöder, F., Popp, A., Hertwich, E.G., Luderer, G.. Understanding future emissions from low-carbon power systems by integration of life-cycle assessment and integrated energy modelling. Nature Energy 2017;2(12):939–945. doi:\bibinfo{doi}{10.1038/s41560-017-0032-9}.

[54] Arvesen, A., Luderer, G., Pehl, M., Bodirsky, B.L., Hertwich, E.G.. Deriving life cycle assessment coefficients for application in integrated assessment modelling. Environmental Modelling & Software 2018;99:111–125. doi:\bibinfo{doi}{10.1016/j.envsoft.2017.09.010}.

[55] Aldersey-Williams, J., Rubert, T.. Levelised cost of energy – a theoretical justification and critical assessment. Energy Policy 2019;124:169–179. doi:\bibinfo{doi}{10.1016/j.enpol.2018.10.004}.

[56] National Renewable Energy Laboratory, . Simple levelized cost of energy (LCOE) calculator documentation. 2019. URL `https://www.nrel.gov/analysis/tech-lcoe-documentation.html`.

[57] Duncan Seddon Associates, . Chemical economics - cracking operations. 2014. URL `http://www.duncanseddon.com/docs/pdf/steam-cracking-operations-forum-docs.pdf`.

[58] Clomburg, J.M., Crumbley, A.M., Gonzalez, R.. Industrial biomanufacturing: The future of chemical production. Science (New York, NY) 2017;355(6320). doi:\bibinfo{doi}{10.1126/science.aag0804}.

[59] Yang, M., You, F.. Comparative techno-economic and environmental analysis of ethylene and propylene manufacturing from wet shale gas and naphtha. Industrial & Engineering Chemistry Research 2017;56(14):4038–4051. doi:\bibinfo{doi}{10.1021/acs.iecr.7b00354}.

[60] Boulamanti, A., Moya, J.A.. Production costs of the chemical industry in the EU and other countries: Ammonia, methanol and light olefins. Renewable and Sustainable Energy Reviews 2017;68:1205–1212. doi:\bibinfo{doi}{10.1016/j.rser.2016.02.021}.

[61] Schmidt, O., Gambhir, A., Staffell, I., Hawkes, A., Nelson, J., Few, S.. Future cost and performance of water electrolysis: An expert elicitation study. International Journal of Hydrogen Energy 2017;42(52):30470–30492. doi:\bibinfo{doi}{10.1016/j.ijhydene.2017.10.045}.

[62] Danish Energy Agency, . Technology data for renewable fuels. ????

[63] Larscheid, P., Lück, L., Moser, A.. Potential of new business models for grid integrated water electrolysis. Renewable Energy 2018;125:599–608. doi:\bibinfo{doi}{10.1016/j.renene.2018.02.074}.

[64] Broehm, M., Strefler, J., Bauer, N.. Techno-economic review of direct air capture systems for large scale mitigation of atmospheric $CO_2$. SSRN Electronic Journal 2015;doi:\bibinfo{doi}{10.2139/ssrn.2665702}.

[65] Open Power System Data, . Data package time series. 2019. doi:\bibinfo{doi}{10.25832/time{\textunderscore}series/2019-06-05}.

[66] Godini, H., Xiao, S., Kim, M., Holst, N., Jašo, S., Görke, O., et al. Experimental and model-based analysis of membrane reactor performance for methane oxidative coupling: Effect of radial heat and mass transfer. Journal of Industrial and Engineering Chemistry 2014;20(4):1993–2002. doi:\bibinfo{doi}{https://doi.org/10.1016/j.jiec.2013.09.022}. URL `https://www.sciencedirect.com/science/article/pii/S1226086X13004425`.

[67] Garcés, D., Díaz, E., Sastre, H., Ordóñez, S., González-LaFuente, J.M.. Evaluation of the potential of different high calorific waste fractions for the preparation of solid recovered fuels. Waste management (New York, NY) 2016;47(Pt B):164–173. doi:\bibinfo{doi}{10.1016/j.wasman.2015.08.029}.

[68] The International Bank for Reconstruction and Development, . Municipal solid waste incineration. 1999.

[69] Finkbeiner, M.. Finkbeiner, m. carbon footprinting—opportunities and threats. The International Journal of Life Cycle Assessment 2009;14(2):91–94. doi:\bibinfo{doi}{10.1007/s11367-009-0064-x}.

[70] de Smedt, P.. Energy demand steam cracking (association of petrochemical producers in europe): Personal conversation (e-mail). 2019.

[71] Worrell, E., Phylipsen, D., Einstein, D., Martin, N.. Energy use and energy intensity of the U.S. chemical industry. 2000.

[72] Ren, T., Daniëls, B., Patel, M.K., Blok, K.. Petrochemicals from oil, natural gas, coal and biomass: Production costs in 2030–2050. Resources, Conservation and Recycling 2009;53(12):653–663. doi:\bibinfo{doi}{10.1016/j.resconrec.2009.04.016}.

[73] Zheng, J., Suh, S.. Strategies to reduce the global carbon footprint of plastics. Nature Climate Change 2019;9(5):374–378. doi:\bibinfo{doi}{10.1038/s41558-019-0459-z}.

[74] Plastics Europe, . Ecoprofiles and environmental declarations – high-density polyethylene (HDPE), low-density polyethylene (LDPE), linear low-density polyethylene (LLDPE). 2014.

[75] Linstrom, P.. NIST chemistry webbook, NIST standard reference database 69. 1997. doi:\bibinfo{doi}{10.18434/T4D303}.

[76] Plastics Europe, . Ecoprofiles and environmental declarations – LCI methodology and PCR for un-compounded polymer resins and reactive polymer precursor (version 2.0, april 2011). 2011.

[77] International Energy Agency, . Tracking industrial energy efficiency and $CO_2$ emissions. 2007.

[78] Umweltbundesamt, . Wirkungsgrad fossiler Kraftwerke [Efficiency of fossil power plants]. 2019. URL `https://www.umweltbundesamt.de/daten/energie/konventionelle-kraftwerke-erneuerbare-energien#textpart-1`.

[79] Leimbach, M., Bauer, N., Baumstark, L., Edenhofer, O.. Mitigation costs in a globalized world: Climate policy analysis with REMIND-R. Environmental Modeling & Assessment 2010;15(3):155–173. doi:\bibinfo{doi}{10.1007/s10666-009-9204-8}.

[80] Trading Economics, . Naphtha - 10 year historical data. 2019. URL `https://tradingeconomics.com/commodity/naphtha`.

[81] Trading Economics, . Crude oil - 10 year historical data. 2019. URL `https://tradingeconomics.com/commodity/crude-oil`.

## Appendix A. Material and Methods

### *Appendix A.1. Theoretical Background*

The following section provides further background information on the technologies considered in this study for reader less familiar with them.

#### *Appendix A.1.1. Steam Cracking (SC)*

SC is the thermal pyrolysis of various oil–derived feedstock to produce ethylene and other HVCs such as propylene and benzene that are used as building blocks in the chemical industry. Additionally, steam cracking produces high–energetic gases ($H_2$ and $CH_4$) and longer-chained and saturated hydrocarbons that are usually fed back to the refinery or exported [32]. The process requires large amounts of heat to reach the cracking temperature of 759°C - 1000°C [11]. This heat is usually subsequently recovered and used in the later steps of fractionating the products [11, 32, 70]. Various feedstocks are employed in steam cracking, with naphtha beeing the most common [32, 71]. The feedstock used influences the product composition with naphtha cracking producing higher shares of other HVCs, hydrogen and methane than other feedstocks such as Ethane. Therefore, it can supply the largest part of its fuel demand by energetically recycling this co—produced methane and hydrogen [32, 72].

#### *Appendix A.1.2. Power-to-Gas (PtG)*

The PtG technology has gained significant traction during the last years as a strategy to produce low-carbon fuels while mitigating the temporal mismatch between electricity supply and demand in energy systems with large shares of renewable sources [7, 16–18, 21]. Besides fostering the integration of renewables, its key strengths are its versatile application in many different sectors such as energy storage, mobility or industry, its ability to use existing natural gas infrastructure to some extent and its high public acceptance [22].

The high electrolyser costs and low system efficiencies of around 55% are the main barriers to a large scale implementation of PtG systems under current economic conditions [17, 22, 23]. However, both are projected to improve in the future, therefore PtG is expected to play a substantial role in many low-emission scenarios [7, 24, 25].

#### *Appendix A.1.3. Oxidative Coupling of Methane (OCM)*

The production of ethylene via oxidative coupling of methane has attracted industrial and academic interests ever since its first introduction in the 1980s [35]. However, the technical implementation is hindered by a low selectivity and a number of undesired side reactions such as the full oxidation of methane, ethane and ethylene to carbon monoxide and $CO_2$, resulting in low ethylene yields. Therefore the search for more selective catalysts is a major area of research in OCM development. A first commercial demonstration plant run by Siluria Technologies in Texas, U.S. has started operation in 2014 [36, 37].

In the light of tighter environmental regulations and concerns over climate change, OCM has also attracted attention due to its potential environmental superiority. Stangland [38] points out that OCM has both a higher thermodynamic and carbon efficiency than steam cracking. Additionally, OCM can utilize biogas as a renewable feedstock [39]. OCM as a CCU process has already been discussed in the mitigation literature to some extent [33, 34] but has so far not been demonstrated technically. Accordingly, it has not yet been subjected to a thorough analysis of its mitigation potential, a gap we want to close with this study.

*Appendix A.2. Product systems, functional unit and process assumptions*

For our product system we assume the steam cracker uses Naphtha as feedstock, with an ethylene yield of $0.3\,\mathrm{t_{Eth}\,t_{Naph}^{-1}}$ [32]. We assume propylene and benzene to be formed as valuable by–products, as well as off–gases ($CH_4$, $H_2$) which are used as fuel in the cracking furnace. In the electrified steam cracker we substitute the gas furnace by an electric furnace. We assume the efficiency of the electric furnace to be identical to that of the gas furnace as no specific data is available.

The OCM–PtG process produces ethylene from the reaction of $H_2$ and $O_2$ after the following equations:

$$8\,H_2O \xrightarrow{e^-} 8\,H_2 + 4\,O_2 \qquad \text{(Electrolysis)} \qquad \text{(A.1)}$$

$$2\,CO_2 + 8\,H_2 \rightleftharpoons 2\,CH_4 + 4\,H_2O \qquad \text{(Methanation)} \qquad \text{(A.2)}$$

$$2\,CH_4 + O_2 \longrightarrow C_2H_4 + 2\,H_2O \qquad \text{(OCM)} \qquad \text{(A.3)}$$

We assume $CO_2$ to be captured directly from the atmosphere through DAC with a technology based on the concept used by ClimeWorks [51], which energy demand can be partly met by waste heat from the methanation and OCM reactions.

In the initial design of the OCM-PtG plant we assume an alkaline electrolyser that is running on constant load with an efficiency $\eta_{el}$ of $0.72\,\mathrm{MWh_{H_2}\,MWh_{el}^{-1}}$ based on Milanzi et al. [24]. The oxygen produced during electrolysis is partly used in the OCM reaction. For the economic analysis we also investigate systems that run in flexible load to take advantage of fluctuating electricity prices. Here we use a polymer electrolyte membrane electrolyser that is better suited for flexible load. The integration of hydrogen storage facilities in the model is beyond the scope of this work and is therefore not taken into account in the flexible systems.

Emissions from the plant construction phase are not considered as these have been shown to be negligible in comparable studies [30]. Upstream emission associated with the catalyst production are also neglected as no data was available and those from transport are not included as the product system lacks sufficient geographical definition. Emissions from (waste) water treatment are neglected in the OCM process since equally detailed data is not available for steam cracking and inclusion would compromise the comparability between the two processes.

Cradle–to–grave emissions also include the life cycle stages of resin production, manufacturing and EoL. Due to the versatile use of ethylene, not all possible fates are modelled. In terms of resin production, PE and PVC production are included, which together make up 70 % of ethylene demand [32]. We chose representative products, for which GaBi datasets are available: PVC pipes, PE bottles and PE foam. From these aggregated datasets, we model the emissions associated with conversion of resins to product as percentages of the total emissions based on Zheng and Suh [73]. For PE, emissions from polymerization are also available from Plastics Europe [74], while for PVC none are provided. EoL strategies included are recycling and incineration. We use GaBi datasets of EoL processes to determine their energy demand, which is then converted to emissions under a given electricity grid carbon intensity. Emission factors for incineration are estimated based on stoichiometric coefficients. We combine each product with each EoL fate to map the solution space of possible downstream product fates for ethylene.

*Appendix A.3. Life Cycle Inventory and Impact Assessment*

For the inventory analysis, we set up energy, mass and carbon flow balances for all main (foreground) processes (depicted bold in Figure 1). From the mass balance we calculate associated emissions by multiplying each flow with its respective emission factor. For direct combustion, we derived these emission factors from Eggleston [43] or based on stoichiometric factors. Electricity demand for all processes is provided by the grid if not specified otherwise. As we investigate the overall emissions dependent on the carbon intensity of electricity, we varied this parameter between $0.4\,\mathrm{t_{CO_2eq}\,MWh^{-1}}$ to $0.0\,\mathrm{t_{CO_2eq}\,MWh^{-1}}$. For all other flows we use data from the life cycle assessment–software GaBi, with the database version 8.7 [45]. We chose EU–28 data where available and country–specific data otherwise. All mass flows, emission factors and their sources are documented in tables Appendix A.2 – Appendix A.4. The carbon content of a compound i is calculated from the molar mass of the carbon in the compound $M_{C,i}$, divided by the molar mass of the compound $M_i$

$$x_C = \frac{M_{C,i}}{M_i} \tag{A.4}$$

with

$$M_{C,i} = n_{C,i} \cdot M_C \tag{A.5}$$

where $n_{C,i}$ is the number of carbon atoms in a molecule of compound i and $M_C = 12\,\mathrm{g\,mol^{-1}}$ is the molar mass of carbon

For multi–compound streams such as naphtha, the Intergovermental Panel on Climate Change (IPCC) gives a carbon content $x_C$ in kg/GJ. This is converted to a mass fraction using the LHV in GJ/t also given by the IPCC [43]:

$$x_{C,i}(mass) = x_{C,i}(energy) \cdot LHV_i \tag{A.6}$$

Table Appendix A.1: Basic data used to set up emission inventories

| $i$ | $M_i$ ($\mathrm{g\,mol^{-1}}$) | $n_{C,i}$ | $x_C$ | $EF_i$ ($\mathrm{t_{CO_2eq}\,t_i^{-1}}$) | $LHV_i$ ($\mathrm{GJ\,t^{-1}}$) | based on |
|---|---|---|---|---|---|---|
| Oxygen atom | 16 | - | - | - | - | Linstrom [75] |
| Hydrogen atom | 1 | - | - | - | - | Linstrom [75] |
| | | | | | | |
| Hydrogen | 2 | - | - | - | 120 | Linstrom [75] |
| Methane | 16 | 1 | 0.750 | 2.60 | 50.0 | Linstrom [75] |
| Carbon Monoxide | 28 | 1 | 0.429 | 1.57 | 10 | Linstrom [75] |
| Carbon Dioxide | 44 | 1 | 0.273 | - | - | Linstrom [75] |
| Ethylene | 28 | 2 | 0.857 | 3.14 | 47.2 | Linstrom [75] |
| Propylene | 42 | 3 | 0.857 | 3.13 | 45.8 | Linstrom [75] |
| Benzene | 78 | 6 | 0.923 | 3.38 | 40.2 | Linstrom [75] |
| | | | | | | |
| Crude Oil | n.a. | n.a. | 0.846 | 3.10 | 42.3 | Eggleston [43] |
| Naphtha | n.a. | n.a. | 0.890 | 3.26 | 44.5 | Eggleston [43] |
| Natural Gas | n.a. | n.a. | n.a. | 2.70 | 48.0 | Eggleston [43] |
| Residual Fuel Oil | n.a. | n.a. | n.a. | 3.13 | 40.4 | Eggleston [43] |

Molar masses and other data relevant for the calculations of inventories are summarized in table Appendix A.1.
After setting up the mass balance, the emissions where calculated as

$$\text{Emissions} = \text{flow} \cdot \text{emissions factor} \tag{A.7}$$

Flows, emission factors and resulting emissions are given in table Appendix A.5 for an exemplary carbon intensity of 0.4 t_CO2/MWh.

Table Appendix A.2: Overview over inventory data for conventional steam cracking

Table Appendix A.2: Conventional Steam Cracking

| Input | | | | | Output | | | | |
|---|---|---|---|---|---|---|---|---|---|
| Flow | $\mathbb{E}$ $\frac{\text{MWh}}{\text{t}_{\text{Eth.}}}$ | $m_i$ $\frac{\text{t}_\text{i}}{\text{t}_{\text{Eth.}}}$ | $m_C$ $\frac{\text{t}_\text{C}}{\text{t}_{\text{Eth.}}}$ | | Flow | $\mathbb{E}$ $\frac{\text{MWh}}{\text{t}_{\text{Eth.}}}$ | $m_i$ $\frac{\text{t}_\text{i}}{\text{t}_{\text{Eth.}}}$ | $m_C$ $\frac{\text{t}_\text{C}}{\text{t}_{\text{Eth.}}}$ | |
| Naphtha | 44.2 | 3.58 | 3.19 | [1] | Ethylene | 13.1 | 1.00 | 0.860 | [1] |
| Electricity | 0.21 | – | – | [2] | Methane (Fuel) | 6.78 | 0.488 | 0.360 | [1] |
| Heat | 6.78 | 0.488 | 0.360 | [3] | Methane (Export) | 0.79 | 0.057 | 0.02 | [1] |
| | | | | | Hydrogen (Export) | 1.10 | 0.032 | – | [1] |
| | | | | | By–Products | 9.42 | 2.03 | 1.97 | [4] |

[1] Flows based on Zimmermann and Walzl [32], upstream emissions from thinkstep [45]
[2] Based on Ren et al. [11], Boulamanti and Moya [60], Plastics Europe [76], upstream emissions from REMIND
[3] No consistent data on heating demand available, calculated as the difference between total and electric energy demand based on Ren et al. [11], Worrell et al. [71], Plastics Europe [76], International Energy Agency [77].
[4] Calculated as difference between mass input and other mass outputs

Table Appendix A.2: System Expansion

| Input | | | | | Output | | | | |
|---|---|---|---|---|---|---|---|---|---|
| Flow | $\mathbb{E}$ $\frac{\text{MWh}}{\text{t}_{\text{Eth.}}}$ | $m_i$ $\frac{\text{t}_\text{i}}{\text{t}_{\text{Eth.}}}$ | $m_C$ $\frac{\text{t}_\text{C}}{\text{t}_{\text{Eth.}}}$ | | Flow | $\mathbb{E}$ $\frac{\text{MWh}}{\text{t}_{\text{Eth.}}}$ | $m$ $\frac{\text{t}_\text{i}}{\text{t}_{\text{Eth.}}}$ | $m_C$ $\frac{\text{t}_\text{C}}{\text{t}_{\text{Eth.}}}$ | |
| Methane | 0.79 | 0.057 | 0.043 | [5] | Electricity | 4.32 | - | - | [8] |
| Hydrogen | 1.10 | 0.032 | — | [6] | | | | | |
| Grid | 3.39 | – | – | [7] | | | | | |

[5] Difference between Methane produced and Methane used as fuel
[6] Exported by steam cracker [7] Upstream emissions from REMIND
[8] $\eta_{conv.}$ of 0.5 in gas–fired power plant for electricity generation [78]

Table Appendix A.3: Overview over inventory data for electrified steam cracking

Table Appendix A.3: Electrified Steam Cracking

| Input | | | | | Output | | | | |
|---|---|---|---|---|---|---|---|---|---|
| Flow | $\mathbb{E}$ $\frac{\text{MWh}}{\text{t}_{\text{Eth.}}}$ | $m_i$ $\frac{\text{t}_\text{i}}{\text{t}_{\text{Eth.}}}$ | $m_C$ $\frac{\text{t}_\text{C}}{\text{t}_{\text{Eth.}}}$ | | Flow | $\mathbb{E}$ $\frac{\text{MWh}}{\text{t}_{\text{Eth.}}}$ | $m_i$ $\frac{\text{t}_\text{i}}{\text{t}_{\text{Eth.}}}$ | $m_C$ $\frac{\text{t}_\text{C}}{\text{t}_{\text{Eth.}}}$ | |
| Naphtha | 44.2 | 3.58 | 3.19 | [1] | Ethylene | 13.1 | 1.00 | 0.860 | [1] |
| Electricity | 6.99 | – | – | [2] | Methane (Fuel) | – | – | – | [1] |
| Electricity (Furnace) | 6.78 | – | – | [3] | Methane (Export) | 7.57 | 0.55 | 0.76 | [1] |
| | | | | | Hydrogen (Export) | 1.10 | 0.032 | – | [1] |
| | | | | | By–Products | 9.42 | 2.03 | 1.97 | [4] |

[1] Flows based on Zimmermann and Walzl [32]
[2] Based on Ren et al. [11], Boulamanti and Moya [60], Plastics Europe [76], upstream emissions from REMIND
[3] Demand and furnace efficiency are assumed to be identical to conventional process
[4] Calculated as difference between mass input and other mass outputs

Table Appendix A.3: System Expansion

| Input | | | | | Output | | | | |
|---|---|---|---|---|---|---|---|---|---|
| Flow | $\mathbb{E}$ $\frac{\text{MWh}}{\text{t}_{\text{Eth.}}}$ | $m_i$ $\frac{\text{t}_\text{i}}{\text{t}_{\text{Eth.}}}$ | $m_C$ $\frac{\text{t}_\text{C}}{\text{t}_{\text{Eth.}}}$ | | Flow | $\mathbb{E}$ $\frac{\text{MWh}}{\text{t}_{\text{Eth.}}}$ | $m$ $\frac{\text{t}_\text{i}}{\text{t}_{\text{Eth.}}}$ | $m_C$ $\frac{\text{t}_\text{C}}{\text{t}_{\text{Eth.}}}$ | |
| Methane | 7.57 | 0.545 | 0.409 | [5] | Electricity | 4.32 | - | - | [6] |
| Hydrogen | 1.10 | 0.032 | - | [5] | | | | | |

[5] Exported by steam cracker
[6] $\eta_{conv.}$ of 0.5 for electricity generation in gas–fired power plant [78]

Table Appendix A.4: Overview over inventory data for OCM–PtG

Table Appendix A.4: OCM–PtG

| Input | | | | | Output | | | | |
|---|---|---|---|---|---|---|---|---|---|
| Flow | $\mathbb{E}$ $\frac{\text{MWh}}{\text{t}_{\text{Eth.}}}$ | $m_i$ $\frac{\text{t}_\text{i}}{\text{t}_{\text{Eth.}}}$ | $m_C$ $\frac{\text{t}_\text{C}}{\text{t}_{\text{Eth.}}}$ | | Flow | $\mathbb{E}$ $\frac{\text{MWh}}{\text{t}_{\text{Eth.}}}$ | $m$ $\frac{\text{t}_\text{i}}{\text{t}_{\text{Eth.}}}$ | $m_C$ $\frac{\text{t}_\text{C}}{\text{t}_{\text{Eth.}}}$ | |
| Hydrogen | 23.2 | 0.694 | - | [1] | Ethylene | 13.1 | 1.98 | 0.857 | [1] |
| $CO_2$ | - | 3.64 | 1.26 | [1] | Methane | 2.53 | 0.183 | 0.137 | [1] |
| Oxygen | - | 1.28 | - | [1] | Hydrogen | 0.207 | 0.008 | - | [1] |
| Electricity | 1.10 | - | - | [1] | Heat | 5.42 | - | - | [1] |
| | | | | | Purge | n.a. | 3.61 | n.a. | [2] |

[1] OCM–PtG Aspen Plus process model
[2] Aspen, water from methanation and $CO_2$ separation, Light gases from distillation

Table Appendix A.4: System Expansion

| Input | | | | | Output | | | | |
|---|---|---|---|---|---|---|---|---|---|
| Flow | $\mathbb{E}$ $\frac{\text{MWh}}{\text{t}_{\text{Eth.}}}$ | $m_i$ $\frac{\text{t}_\text{i}}{\text{t}_{\text{Eth.}}}$ | $m_C$ $\frac{\text{t}_\text{C}}{\text{t}_{\text{Eth.}}}$ | | Flow | $\mathbb{E}$ $\frac{\text{MWh}}{\text{t}_{\text{Eth.}}}$ | $m$ $\frac{\text{t}_\text{i}}{\text{t}_{\text{Eth.}}}$ | $m_C$ $\frac{\text{t}_\text{C}}{\text{t}_{\text{Eth.}}}$ | |
| Methane | 2.53 | 0.183 | 0.137 | [6] | Electricity | 4.32 | – | – | [8] |
| Hydrogen | 0.270 | 0.009 | - | [6] | | | | | |
| Grid | 2.89 | – | - | | | | | | |
| Propylene | 7.0 | 0.55 | 0.472 | [7] | Propylene | 7.0 | 0.55 | 0.472 | [7] |
| Benzene | 3.1 | 0.267 | 0.246 | [7] | Benzene | 3.1 | 0.267 | 0.246 | [7] |

[6] purged by OCM plant [7] [45]
[8]$\eta_{conv.}$ of 0.5 for electricity generation [78]

Table Appendix A.4: Electrolysis

| Input | | | | | Output | | | | |
|---|---|---|---|---|---|---|---|---|---|
| Flow | $\mathbb{E}$ $\frac{\text{MWh}}{\text{t}_{\text{Eth.}}}$ | $m_i$ $\frac{\text{t}_\text{i}}{\text{t}_{\text{Eth.}}}$ | $m_C$ $\frac{\text{t}_\text{C}}{\text{t}_{\text{Eth.}}}$ | | Flow | $\mathbb{E}$ $\frac{\text{MWh}}{\text{t}_{\text{Eth.}}}$ | $m$ $\frac{\text{t}_\text{i}}{\text{t}_{\text{Eth.}}}$ | $m_C$ $\frac{\text{t}_\text{C}}{\text{t}_{\text{Eth.}}}$ | |
| Electricity | 32.2 | - | - | [9] | Hydrogen | 23.2 | 0.694 | - | |
| Water | – | 7.49 | – | | Oxygen | – | 6.66 | | [10] |

[9] efficiency of 0.72 $\text{MWh}_{\text{H}_2}\,\text{MWh}_{\text{el}}^{-1}$ is assumed based on Milanzi et al. [24]
[10] own stoichiometric calculation

Table Appendix A.5: Flows, emission factors and exemplary results for emissions with carbon intensity $x = 0.4 \frac{t_{CO_2 eq}}{MWh}$

Table Appendix A.5: Conventional Steam Cracking

| Flow | Quantity | Unit | EF | Unit | Emissions $\frac{t_{CO_2 eq}}{t_{Eth.}}$ | Carbon flow $\frac{t_C}{t_{Eth.}}$ |
|---|---|---|---|---|---|---|
| Electricity | 0.210 | $\frac{MWh}{t_{Eth.}}$ | $x$ | $\frac{t_{CO_2 eq}}{MWh}$ | 0.084 | 0.023 |
| Heat | 0.488 | $\frac{t}{t_{Eth.}}$ | 2.6 | $\frac{t_{CO_2 eq}}{t_{Eth.}}$ | 1.27 | 0.343 |
| System Expansion (EL) | 3.39 | $\frac{MWh}{t_{Eth.}}$ | $x$ | $\frac{t_{CO_2 eq}}{MWh}$ | 1.35 | 0.36 |
| System Expansion (HO) | 3.39 | $\frac{MWh}{t_{Eth.}}$ | 0.310 | $\frac{t_{CO_2 eq}}{MWh}$ | 1.06 | 0.286 |
| System Expansion (NG) | 3.39 | $\frac{MWh}{t_{Eth.}}$ | 0.244 | $\frac{t_{CO_2 eq}}{MWh}$ | 0.829 | 0.224 |
| Refinery | 3.58 | $\frac{t}{t_{Eth.}}$ | 0.535 | $\frac{t_{CO_2 eq}}{t_{Eth.}}$ | 1.92 | 0.517 |
| Methane | 0.06 | $\frac{t}{t_{Eth.}}$ | 2.6 | $\frac{t_{CO_2 eq}}{t_{Eth.}}$ | 0.140 | 0.038 |
| By-Products | – | | – | | – | |
| Electrolyser | – | | – | | – | |
| Carbon Capture | – | | – | | – | |

Table Appendix A.5: Electrified Steam Cracking

| Flow | Quantity | Unit | EF | Unit | Emissions $\frac{t_{CO_2 eq}}{t_{Eth.}}$ | Carbon flow $\frac{t_C}{t_{Eth.}}$ |
|---|---|---|---|---|---|---|
| Electricity | 6.99 | $\frac{MWh}{t_{Eth.}}$ | $x$ | $\frac{t_{CO_2 eq}}{MWh}$ | 2.97 | 0.75 |
| Heat | – | | – | | – | |
| System Expansion | – | | – | | – | |
| Refinery | 3.58 | $\frac{t}{t_{Eth.}}$ | 0.535 | $\frac{t_{CO_2 eq}}{t_{Eth.}}$ | 1.92 | 0.517 |
| Methane | 0.545 | $\frac{t}{t_{Eth.}}$ | 2.6 | $\frac{t_{CO_2 eq}}{t_{Eth.}}$ | 1.42 | 0.383 |
| By-Products | – | | – | | – | |
| Electrolyser | – | | – | | – | |
| Carbon Capture | – | | – | | – | |

Table Appendix A.5: (cont.) Flows, emission factors and exemplary results for emissions with carbon intensity $x = 0.4 \frac{t_{CO_2 eq}}{MWh}$

Table Appendix A.5: OCM

| Name | Flow | Unit | EF | Unit | Emissions $\frac{t_{CO_2 eq}}{t_{Eth.}}$ | Carbon flow $\frac{t_C}{t_{Eth.}}$ |
|---|---|---|---|---|---|---|
| Electricity | 1.1 | $\frac{MWh}{t_{Eth.}}$ | $x$ | $\frac{t_{CO_2 eq}}{MWh}$ | 0.44 | 0.119 |
| Heat | – | | – | | – | |
| System Expansion | 2.46 | $\frac{MWh}{t_{Eth.}}$ | $x$ | $\frac{t_{CO_2 eq}}{MWh}$ | 0.980 | 0.264 |
| Refinery | – | | – | | – | |
| Methane | 0.183 | $\frac{t}{t_{Eth.}}$ | 2.6 | $\frac{t_{CO_2 eq}}{t_{Eth.}}$ | 0.476 | 0.129 |
| By-Products | 1 | $\frac{t}{t_{Eth.}}$ | 0.623 | $\frac{t_{CO_2 eq}}{t_{Eth.}}$ | 0.623 | 0.168 |
| Electrolyser | 32.2 | $\frac{MWh}{t_{Eth.}}$ | $x$ | $\frac{t_{CO_2 eq}}{MWh}$ | 12.9 | 3.48 |
| Carbon Capture | 4.64 | $\frac{MWh}{t_{Eth.}}$ | $-1 + 1.47 \cdot x$ | $\frac{t_{CO_2 eq}}{MWh}$ | −1.91 | −0.516 |

Table Appendix A.6: Overview over datasets taken from GaBi

| Stream | modelled as | type | region |
|---|---|---|---|
| Benzene | Benzene [*] | agg | DE |
| Biomethane | Biomethane from maize silage [**] | agg | EU–28 |
| Heating Oil | Heavy fuel oil (EN15804 B6) | agg | DE |
| Incineration | Waste incineration (plastics) | t–agg | DE |
| Naphtha | Naphtha at refinery | agg | EU–28 |
| Natural Gas | Natural gas | agg | Europe |
| PE bottle | Polyethylene bottle (PE–LD) | agg | Europe |
| PE foam | Polyethylene foam (EN15804 A1–A3) | agg | EU–28 |
| Plastic recycling | Washing (plastic recycling) | e–ep | DE |
| Propylene | Propylene at refinery | agg | EU–28 |
| PVC pipe | Polyvinylchloride pipe (PVC) | agg | Europe |

[*] hydrodealkylation, from toluene and hydrogen, single route

[**] $x_{CH_4} = 97.8\,\%$, $x_C = 74.9\,\%$, $LHV = 48.9\,\mathrm{MJ\,kg^{-1}}$

*Appendix A.4. REMIND*

REMIND is a multi–regional, hybrid model, that combines a top–down core economic module to accounts for an optimal distribution of resources in the economy with a detailed, bottom–up energy systems and a simple climate model [79]. It maximises inter–temporal welfare represented as gross domestic product and determined by the input factors capital, labour and end–use energy for 11 world regions. The energy system module comprises around 50 energy conversion technologies, optimizes the cost for providing the final energy demand requested by the macroeconomic module and feeds the energy system cost back to the overall economic budget constraint. The amount and composition of final energy demand is determined by a market equilibrium between marginal utility and marginal costs of energy use. Technologies are constrained by their capacities, which can in turn be increased by investments. Regional potentials for renewable energy ressources and reserves for exhaustible ressources are provided as exogenous variables.

The time period covered by the model output is from 2005 to 2100, and is resolved in 5–year steps from 2005 until 2060 and ten–year–steps from 2060 to 2100. REMIND also provides life–cycle–emissions of electricity generation until 2050, based on the methodology provided by Pehl et al. [53] and Arvesen et al. [54]. For the Base scenario one should keep in mind that electricity emissions after 2050 are underestimating the life–cycle emissions. For the policy scenarios this is not an issue, as indirect emissions have converged to almost zero by this time.

*Appendix A.5. Costs*

We model naphtha prices following crude oil prices based on a linear regression model shown in Figure Appendix A.2, using historical data taken from Trading Economics [80, 81]

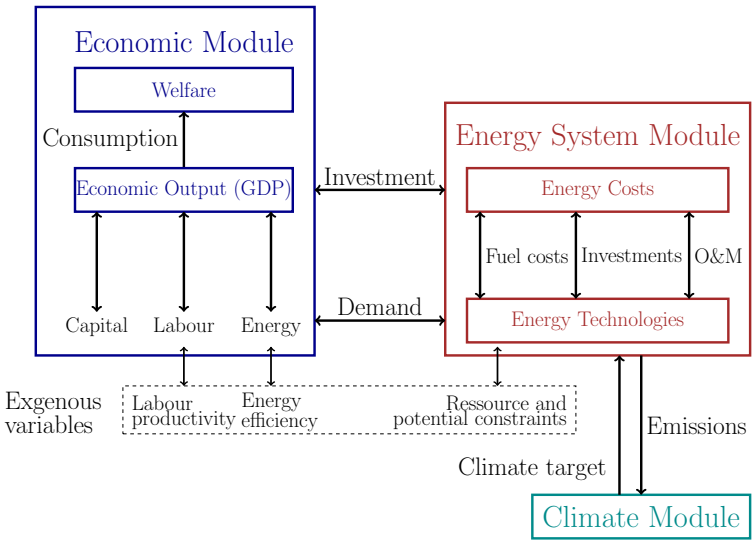


Figure Appendix A.1: Schematic overview over the REMIND model structure. Economic activity creates demand for final energy, which in turn is an input factor to the economy together with capital and labour. Emissions from the energy systems module feed back to the climate system while the climate model determines the bio-physical basis of the economy through ressource constraints and climate targets. Figure adapted from Leimbach et al. [79]

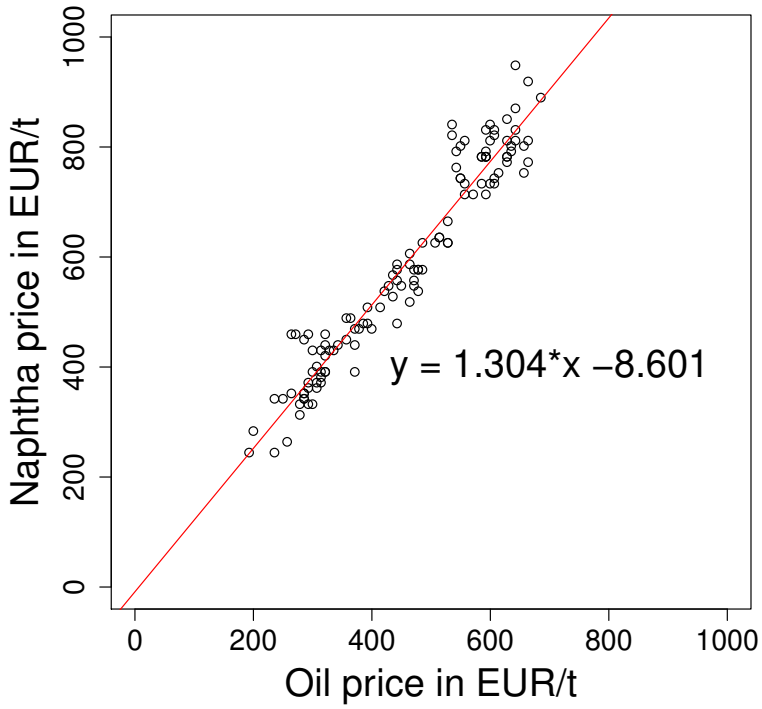


Figure Appendix A.2: Correlation between crude oil and naphtha price.

## Appendix B. Aspen Model

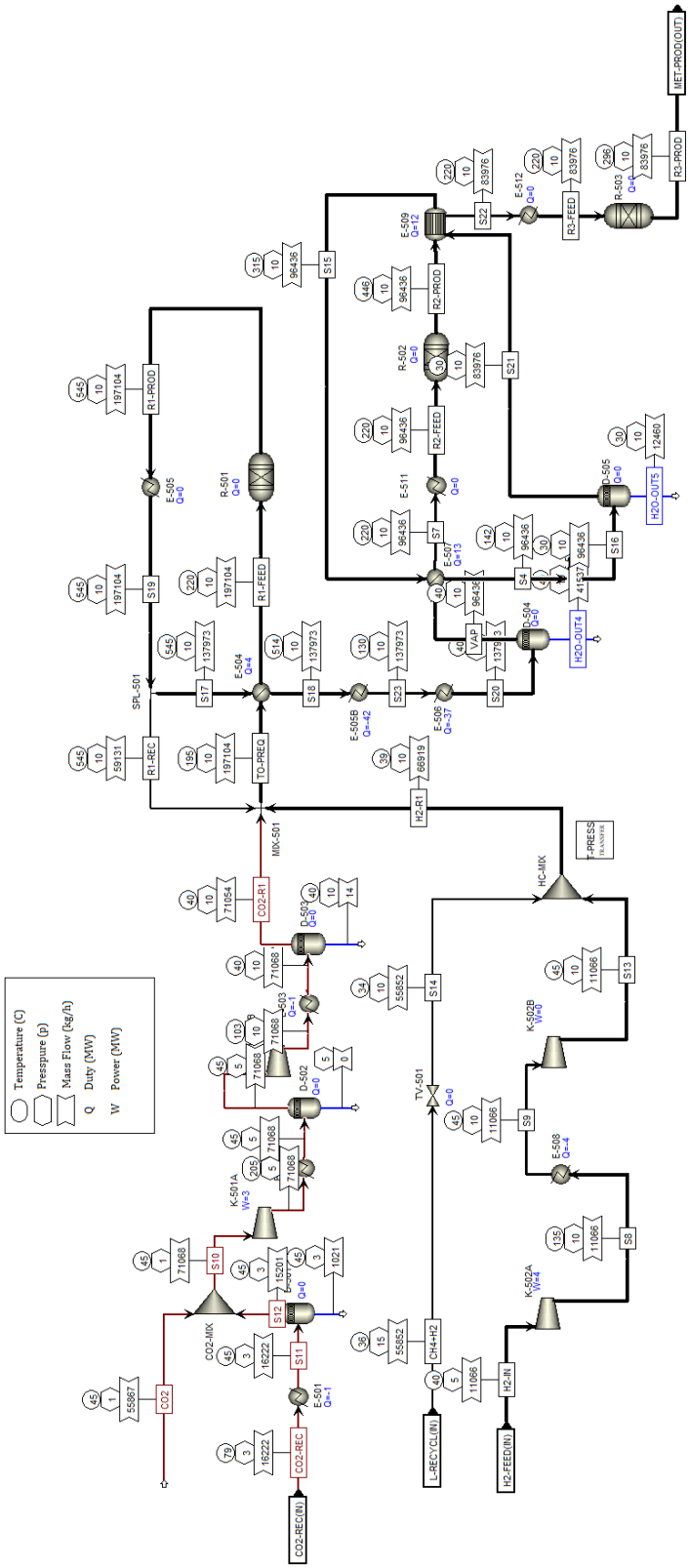


Figure Appendix B.1: Methanation sub–flowsheet

Table Appendix B.1: Stream results for methanation block as in figure Appendix B.1

| | Inflows | | | | Outflows | | | | | |
|---|---|---|---|---|---|---|---|---|---|---|
| | CO2 | CO2-REC | CH4+H2 | H2-IN | H2O-OUT1 | H2O-OUT1 | H2O-OUT3 | H2O-OUT4 | H2O-OUT5 | R3-PROD |
| From | | | | | D-501 | D-501 | D-503 | D-504 | D-505 | R-503 |
| To | CO2-MIX | E-501 | TV-501 | K-502A | | | | | | |
| Temperature in °C | 45 | 78.64696 | 35.78832 | 40 | 45 | 45 | 40 | 40 | 30 | 295.6101 |
| Pressure in bar | 1 | 2.5 | 15 | 5 | 2.5 | 2.5 | 10.01 | 10.01 | 10.01 | 10.01 |
| Mole Flows in kmol h$^{-1}$ | 1269.424 | 414.9526 | 4496.944 | 5280 | 56.66812 | 56.66812 | 0.772033 | 2305.624 | 691.6474 | 5220.436 |
| H2 | 0 | 1.563351 | 1171.745 | 5253.6 | 1.94E-07 | 1.94E-07 | 2.06E-09 | 0.001687 | 0.000115 | 54.70962 |
| N2 | 0 | 0.00817 | 11.45478 | 0 | 6.79E-10 | 6.79E-10 | 6.79E-12 | 6.61E-06 | 1.70E-06 | 11.4619 |
| O2 | 0 | 9.47E-34 | 0 | 0 | 0 | 0 | 0 | 0 | 0 | 2.12E-36 |
| CH4 | 0 | 5.329074 | 3313.101 | 0 | 3.57E-06 | 3.57E-06 | 3.64E-08 | 0.021125 | 0.006278 | 4915.659 |
| C2H4 | 0 | 2.40032 | 0.520181 | 0 | 2.52E-06 | 2.52E-06 | 2.48E-08 | 7.82E-09 | 3.61E-10 | 1.02E-06 |
| C2H6 | 0 | 0.019534 | 9.29E-08 | 0 | 1.44E-08 | 1.44E-08 | 1.39E-10 | 1.37E-06 | 4.01E-07 | 0.123535 |
| C3H6 | 0 | 5.60E-47 | 1.24E-24 | 0 | 0 | 0 | 0 | 9.16E-12 | 6.13E-13 | 6.14E-09 |
| CO | 0 | 0.000118 | 0.12218 | 0 | 7.82E-12 | 7.82E-12 | 7.83E-14 | 4.01E-05 | 1.11E-06 | 0.083947 |
| CO2 | 1269.424 | 336.9126 | 0 | 0 | 0.002198 | 0.002198 | 0.000112 | 0.020266 | 0.001801 | 14.72562 |
| H2O | 0 | 68.71947 | 0 | 26.4 | 56.66591 | 56.66591 | 0.771921 | 2305.581 | 691.6392 | 223.6723 |
| Mass Flows in kg h$^{-1}$ | 55867.08 | 16222.26 | 55852.29 | 11066.23 | 1020.949 | 1020.949 | 13.91129 | 41536.92 | 12460.25 | 83975.78 |
| H2 | 0 | 3.151528 | 2362.098 | 10590.63 | 3.92E-07 | 3.92E-07 | 4.15E-09 | 0.003401 | 0.000232 | 110.288 |
| N2 | 0 | 0.228865 | 320.8881 | 0 | 1.90E-08 | 1.90E-08 | 1.90E-10 | 0.000185 | 4.75E-05 | 321.0876 |
| O2 | 0 | 3.03E-32 | 0 | 0 | 0 | 0 | 0 | 0 | 0 | 6.77E-35 |
| CH4 | 0 | 85.49305 | 53151.29 | 0 | 5.73E-05 | 5.73E-05 | 5.83E-07 | 0.338907 | 0.100717 | 78860.74 |
| C2H4 | 0 | 67.33801 | 14.59303 | 0 | 7.08E-05 | 7.08E-05 | 6.97E-07 | 2.19E-07 | 1.01E-08 | 2.85E-05 |
| C2H6 | 0 | 0.587383 | 2.79E-06 | 0 | 4.33E-07 | 4.33E-07 | 4.18E-09 | 4.11E-05 | 1.21E-05 | 3.714646 |
| C3H6 | 0 | 2.36E-45 | 5.22E-23 | 0 | 0 | 0 | 0 | 3.86E-10 | 2.58E-11 | 2.59E-07 |
| CO | 0 | 0.0033 | 3.422323 | 0 | 2.19E-10 | 2.19E-10 | 2.19E-12 | 0.001123 | 3.10E-05 | 2.351398 |
| CO2 | 55867.08 | 14827.46 | 0 | 0 | 0.096744 | 0.096744 | 0.004926 | 0.891883 | 0.07926 | 648.0717 |
| H2O | 0 | 1238 | 0 | 475.6034 | 1020.852 | 1020.852 | 13.90637 | 41535.69 | 12460.07 | 4029.52 |

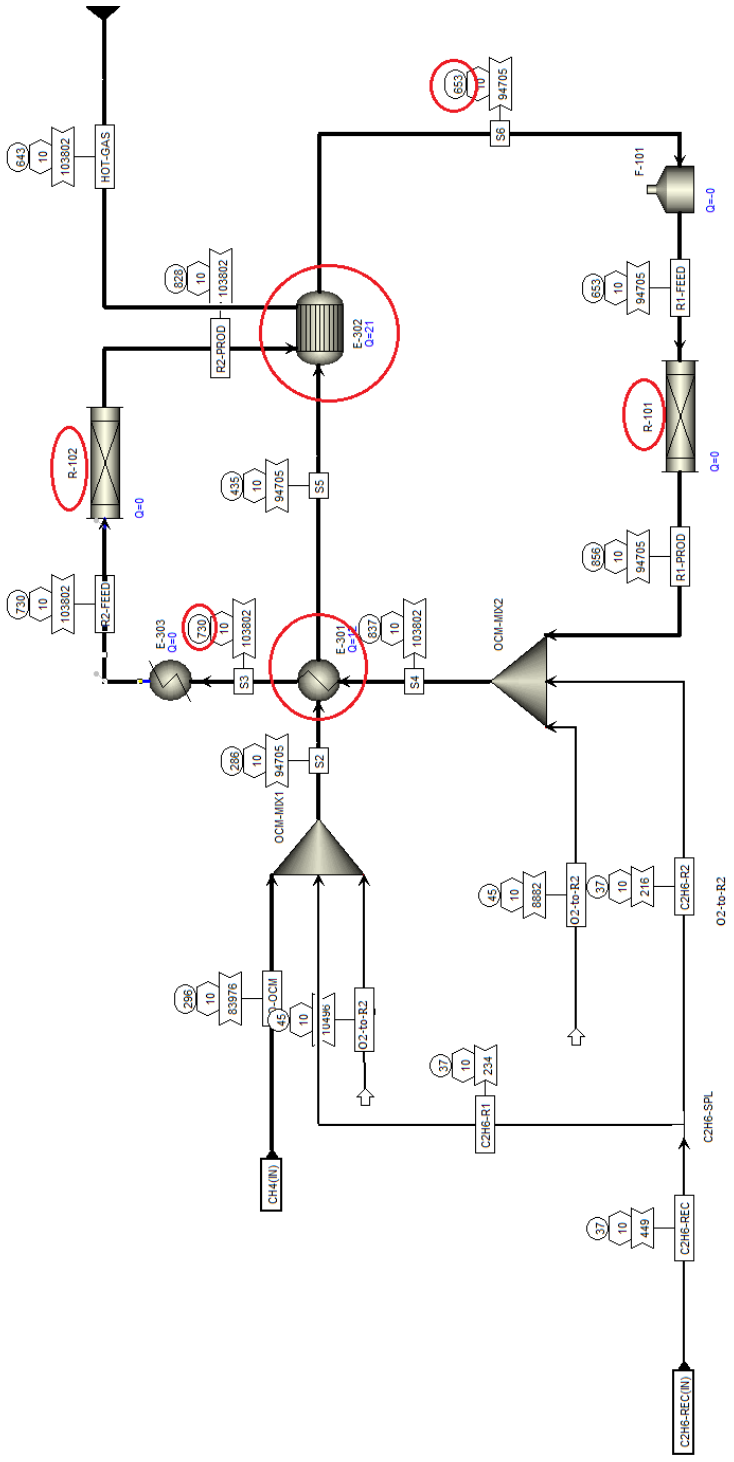


Figure Appendix B.2: OCM sub–flowsheet. Red circles show module most important for regulation of emissions within the process

Table Appendix B.2: Stream results for OCM block as in figure Appendix B.2

| | Inflows | | | | Outflow |
|---|---|---|---|---|---|
| | TO-OCM | C2H6-REC | O2-TO-R1 | O2-TO-R2 | OCM-GAS |
| From | | | | | E-302 |
| To | MIX1 | MIX1/2 | MIX1 | MIX2 | |
| Temperature in °C | 295.6089 | 36.99989 | 45 | 45 | 200 |
| Pressure in bar | 10 | 10 | 10 | 10 | 10 |
| Mole Flows in kmol $h^{-1}$ | 5220.436 | 14.94154 | 328.0387 | 277.5962 | 6431.096 |
| H2 | 54.70962 | 0 | 0 | 0 | 1234.998 |
| N2 | 11.4619 | 0 | 0.328039 | 0.277596 | 12.06695 |
| O2 | 2.12E-36 | 0 | 327.7106 | 277.3186 | 0 |
| CH4 | 4915.659 | 2.36E-47 | 0 | 0 | 3492.81 |
| C2H4 | 1.02E-06 | 0.014365 | 0 | 0 | 549.99 |
| C2H6 | 0.123535 | 14.9266 | 0 | 0 | 15.21436 |
| C3H6 | 6.14E-09 | 0.000577 | 0 | 0 | 0.000577 |
| CO | 0.083947 | 0 | 0 | 0 | 0.12873 |
| CO2 | 14.72562 | 0 | 0 | 0 | 337.2498 |
| H2O | 223.6723 | 0 | 0 | 0 | 788.6374 |
| MEA | 6.01E-20 | 0 | 0 | 0 | 6.01E-20 |
| Mass Flows in kg $h^{-1}$ | 83975.78 | 449.2647 | 10495.54 | 8881.638 | 103802.2 |
| H2 | 110.288 | 0 | 0 | 0 | 2489.608 |
| N2 | 321.0876 | 0 | 9.189504 | 7.776435 | 338.0372 |
| O2 | 6.77E-35 | 0 | 10486.35 | 8873.861 | 0 |
| CH4 | 78860.74 | 3.79E-46 | 0 | 0 | 56034.3 |
| C2H4 | 2.85E-05 | 0.402981 | 0 | 0 | 15429.29 |
| C2H6 | 3.714646 | 448.8374 | 0 | 0 | 457.4903 |
| C3H6 | 2.59E-07 | 0.024278 | 0 | 0 | 0.024288 |
| CO | 2.351398 | 0 | 0 | 0 | 3.605787 |
| CO2 | 648.0717 | 0 | 0 | 0 | 14842.3 |
| H2O | 4029.52 | 0 | 0 | 0 | 14207.52 |
| MEA | 3.67E-18 | 0 | 0 | 0 | 3.67E-18 |

Table Appendix B.3: Stream results for $CO_2$ removal section as in figure **??**

| | Inflow | Outflows | | |
|---|---|---|---|---|
| | OCM-GAS | TO-DIST | H2O-OUT | CO2-OUT |
| From | OCM | CO2-REM | CO2-REM | CO2-REM |
| To | CO2-REM | DIST | | CO2-SPL |
| Temperature in °C | 200 | 45 | 200 | 78.64697 |
| Pressure in bar | 10 | 10 | 10 | 2.5 |
| | | | | |
| Mole Flows in $\mathrm{kmol\,h^{-1}}$ | 6431.096 | 5295.837 | 720.3056 | 414.9526 |
| H2 | 1234.998 | 1233.416 | 0.019029 | 1.563351 |
| N2 | 12.06695 | 12.05872 | 0.000109 | 0.00817 |
| CH4 | 3492.81 | 3487.48 | 0 | 5.329074 |
| C2H4 | 549.99 | 547.5587 | 0.03099 | 2.40032 |
| C2H6 | 15.21436 | 15.19456 | 0.000255 | 0.019534 |
| C3H6 | 0.000577 | 0.000576 | 1.12E-06 | 0 |
| CO | 0.12873 | 0.128611 | 1.56E-06 | 0.000118 |
| CO2 | 337.2498 | 0 | 0.33725 | 336.9126 |
| H2O | 788.6374 | 0 | 719.9179 | 68.71949 |
| MEA | 6.01E-20 | 0 | 0 | 0 |
| | | | | |
| Mass Flows in $\mathrm{kg\,h^{-1}}$ | 103802.2 | 74594.64 | 12985.28 | 16222.26 |
| H2 | 2489.608 | 2486.418 | 0.03836 | 3.151528 |
| N2 | 338.0372 | 337.8068 | 0.003049 | 0.228864 |
| CH4 | 56034.3 | 55948.81 | 0 | 85.49305 |
| C2H4 | 15429.29 | 15361.08 | 0.869394 | 67.33801 |
| C2H6 | 457.4903 | 456.8949 | 0.007668 | 0.587384 |
| C3H6 | 0.024288 | 0.024259 | 4.70E-05 | 0 |
| CO | 3.605787 | 3.602445 | 4.37E-05 | 0.0033 |
| CO2 | 14842.3 | 0 | 14.8423 | 14827.46 |
| H2O | 14207.52 | 0 | 12969.52 | 1238.001 |
| MEA | 3.67E-18 | 0 | 0 | 0 |

Table Appendix B.4: Stream results for light splitter as in figure **??**

| | Inflow | Outflows | |
|---|---|---|---|
| | LIGHTS | L-RECYCL | L-PURGE |
| From | DIST | L-SPLIT | L-SPLIT |
| To | L-SPLIT | METHANAT | |
| Temperature in °C | 35.78832 | 35.78832 | 35.78832 |
| Pressure in bar | 15 | 15 | 15 |
| | | | |
| Mole Flows in kmol $h^{-1}$ | 4733.625 | 4496.944 | 236.6812 |
| H2 | 1233.416 | 1171.745 | 61.6708 |
| N2 | 12.05766 | 11.45478 | 0.602883 |
| CH4 | 3487.475 | 3313.101 | 174.3738 |
| C2H4 | 0.547559 | 0.520181 | 0.027378 |
| C2H6 | 9.78E-08 | 9.29E-08 | 4.89E-09 |
| C3H6 | 1.31E-24 | 1.24E-24 | 6.53E-26 |
| CO | 0.128611 | 0.12218 | 0.006431 |
| | | | |
| Mass Flows (kg $h^{-1}$) | 58791.89 | 55852.29 | 2939.594 |
| H2 | 2486.418 | 2362.098 | 124.3209 |
| N2 | 337.777 | 320.8881 | 16.88885 |
| CH4 | 55948.73 | 53151.29 | 2797.436 |
| C2H4 | 15.36108 | 14.59303 | 0.768054 |
| C2H6 | 2.94E-06 | 2.79E-06 | 1.47E-07 |
| C3H6 | 5.50E-23 | 5.22E-23 | 2.75E-24 |
| CO | 3.602446 | 3.422323 | 0.180122 |

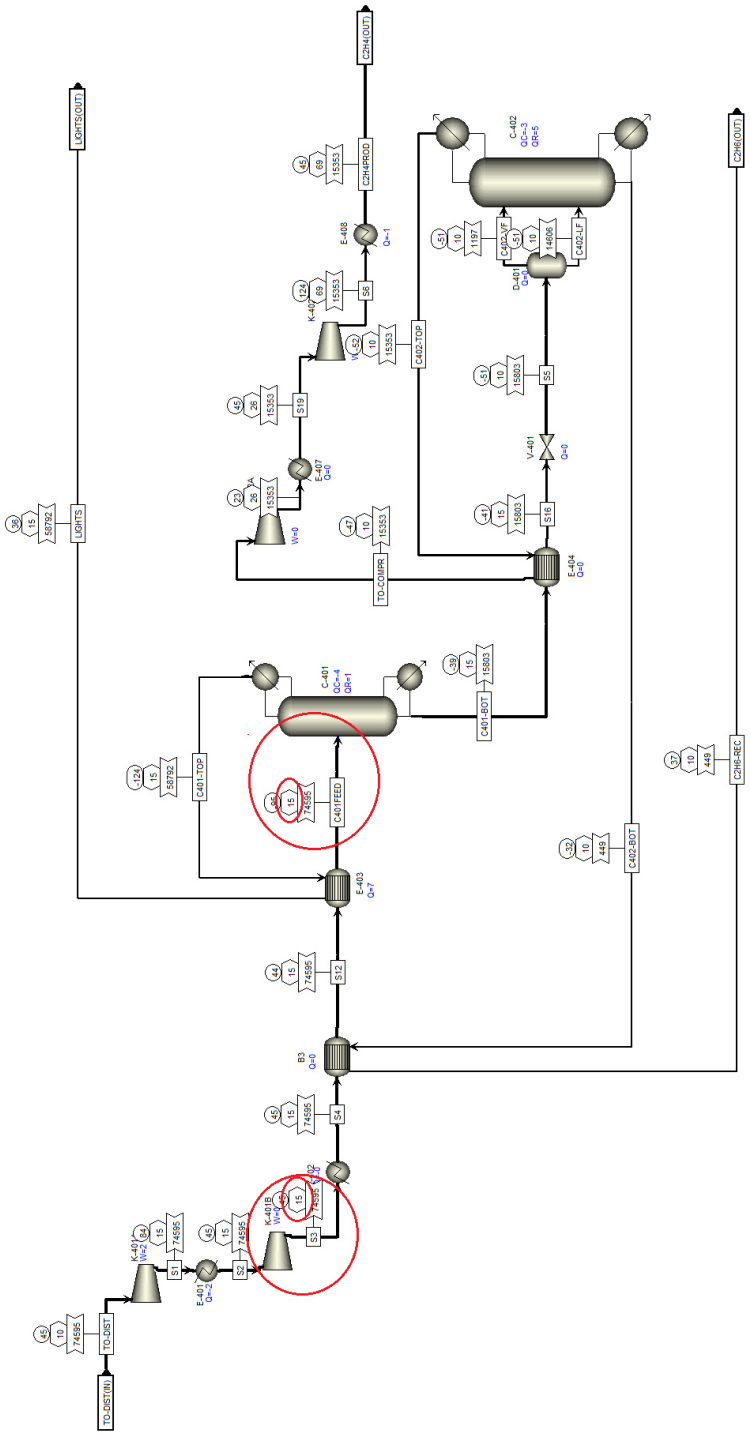


Figure Appendix B.3: Distillation sub–flowsheet. Red circles show module most important for regulation of emissions within the process

Table Appendix B.5: Stream results for distillation block as in figure Appendix B.3

| | Inflow | Outflows | | |
|---|---|---|---|---|
| | TO-DIST | LIGHTS | C2H4PROD | C2H6-REC |
| From | | E-403 | E-408 | B3 |
| To | K-401A | | | |
| Temperature in °C | 44.99999871 | 35.78831663 | 45 | 36.99989444 |
| Pressure in bar | 10 | 15 | 69 | 10 |
| | | | | |
| Mole Flows in kmol $h^{-1}$ | 5295.837374 | 4733.624882 | 547.2702637 | 14.94153916 |
| H2 | 1233.415853 | 1233.415917 | 0 | 0 |
| N2 | 12.05872457 | 12.05765838 | 0 | 0 |
| CH4 | 3487.480313 | 3487.475137 | 0.005622117 | 2.36E-47 |
| C2H4 | 547.5587359 | 0.547558691 | 546.9966286 | 0.014364606 |
| C2H6 | 15.19455988 | 9.78E-08 | 0.268013014 | 14.92659762 |
| C3H6 | 0.000576492 | 1.31E-24 | 6.67E-22 | 5.77E-04 |
| CO | 0.128610992 | 0.128611003 | 0 | 0 |
| | | | | |
| Mass Flows in kg $h^{-1}$ | 74594.63786 | 58791.88561 | 15353.46139 | 449.2646757 |
| H2 | 2486.41835 | 2486.418478 | 0 | 0 |
| N2 | 337.8068396 | 337.7769719 | 0 | 0 |
| CH4 | 55948.80966 | 55948.72663 | 0.090194271 | 3.79E-46 |
| C2H4 | 15361.08136 | 15.3610801 | 15345.31214 | 0.402981199 |
| C2H6 | 456.8949454 | 2.94E-06 | 8.059054846 | 448.8374167 |
| C3H6 | 0.024259138 | 5.50E-23 | 2.80E-20 | 2.43E-02 |
| CO | 3.602445333 | 3.602445628 | 0 | 0 |